HHS Public Access

Author manuscript

J Control Release. Author manuscript; available in PMC 2021 July 10.

Published in final edited form as:

J Control Release. 2020 July 10; 323: 161–178. doi:10.1016/j.jconrel.2020.04.012.

Long-term glycemic control and prevention of diabetes complications *in vivo* using oleic acid-grafted-chitosan-zinc-insulin complexes incorporated in thermosensitive copolymer

Divya Sharma[†], **Jagdish Singh**[†,*]

[†]Department of Pharmaceutical Sciences, School of Pharmacy, College of Health Professions, North Dakota State University, Fargo 58105, ND, USA

Abstract

Daily injections for basal insulin therapy are far from ideal resulting in hypo/hyperglycemic episodes associated with fatal complications in type-1 diabetes patients. Here we report a delivery system that provides controlled release of insulin closely mimicking physiological basal insulin requirement for an extended period following a single subcutaneous injection. Stability of insulin was significantly improved by formation of zinc-insulin hexamers, further stabilized by electrostatic complex formation with chitosan polymer. Insulin complexes were homogenously incorporated into PLA-PEG-PLA, a biodegradable thermogel copolymer, that instantaneously forms a subcutaneous gel-depot following injection. Chitosan polymer was hydrophobically modified using oleic acid prior to complex formation with insulin to enable distribution of oleic acid-grafted-chitosan-zinc-insulin complexes into the hydrophobic core of PLA-PEG-PLA thermogel-copolymer micelles. *In vivo*, daily administration of marketed long-acting insulin, glargine, resulted in fluctuating blood glucose levels between 91 – 443 mg/dL in type 1 diabetic rats. However, single administration of thermogel copolymeric formulation successfully demonstrated slow diffusion of insulin complexes maintaining peak-free basal insulin level of 21 mU/L for 91 days. Sustained release of basal insulin also correlated with efficient glycemic control (blood glucose <120 mg/dL), prevention of diabetic ketoacidosis and absence of cataract development, unlike other treatment groups. Moreover, there was no sign of inflammation, tissue

[*]Author to whom correspondence should be addressed: Department of Pharmaceutical Sciences, School of Pharmacy, College of Health Professions, North Dakota State University, Fargo 58105, ND, USA; jagdish.singh@ndsu.edu; Tel.: +1-701-231-7943; Fax: +1-701-231-8333.

CRediT author statement

Divya Sharma and Jagdish Singh: Conceptualization, Methodology, Writing-Review and Editing; Divya Sharma: Investigation, Validation, Writing-Original Draft Preparation; Jagdish Singh: Supervision, Funding Acquisition.

Disclosure

Authors have no competing interests to declare.

Appendix A

Supplementary data to this article including phase transition of thermosensitive copolymer (Figure S1), ^{1}H NMR (Figure S2) and FT-IR (Figure S3) spectra of chitosan oligosaccharide (CSO, 5 kDa) and oleic acid grafted CSO polymers, and secondary structure estimation of insulin (Table S1).

Data availability

The raw data required to reproduce these findings are available to request from jagdish.singh@ndsu.edu.

damage, or collagen deposition around depot site, suggesting exceptional biocompatibility of the formulation for long-term use.

Graphical Abstract

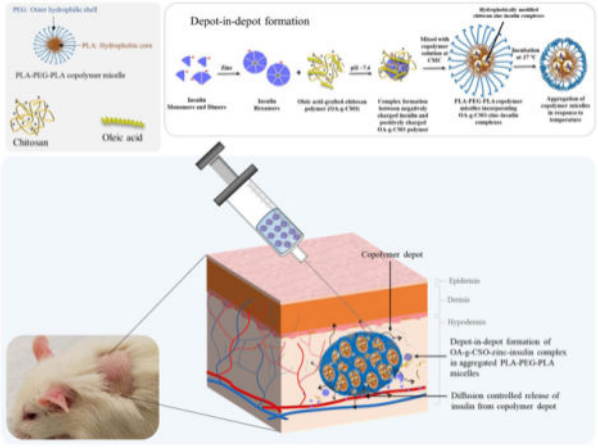

Keywords

controlled release; thermosensitive copolymer; hydrophobic modification; basal insulin; protein stability; glycemic control; prevention of diabetes complications

1. Introduction

Diabetes mellitus (DM) is a chronic progressive metabolic syndrome characterized by hyperglycemia, coming about because of relative or total insufficiency of insulin. Type 1 DM accounts for 5 – 10% of total DM cases worldwide and occurs due to slow and progressive autoimmune destruction of insulin-producing pancreatic β-cells leading to an absolute deficiency of insulin production. Type 2 DM results from decreased function of insulin on insulin-responsive tissues due to insulin resistance, and/or insufficient insulin secretion due to continuing β-cell dysfunction or loss. Insulin replacement therapy using appropriate delivery systems, along with continuous glucose monitoring is crucial for people living with type 1 diabetes and eventually for type 2 diabetes patients, when their treatment is inadequate using oral hypoglycemic agents. Under normal conditions, pancreatic β-cells secrete 0.5 – 1 U of insulin per hour during fasting (basal) state [1]. This enables insulin-dependent entry of glucose into the cells and prevents uncontrolled hydrolysis of triglycerides, limits gluconeogenesis, and modulates energy production overnight as well as for period in-between meals. Basal insulin production accounts for over 50% of daily insulin secretion and corresponding to 3 – 15 mIU/L of fasting insulin concentration [2]. Basal insulin requirement in type-1 DM is currently approached using insulin pump therapy or once/twice daily disposable devices which are accompanied by injection-associated pain, discomfort, increased risk of infection as well as psychological and economical stress for patients and their families [3]. Moreover, none of these devices can deliver insulin at a basal level at a steady rate for more than a day [4]. Recently, researchers working on developing

daily or weekly insulin delivery systems have had some success, but their translation to clinical practice is burdened with challenges such as cost, patient compliance, reproducibility and most importantly stability of insulin [5–7].

To date, subcutaneous route of insulin administration using pumps and pens are the most popular route for insulin therapy. Clinical and investigational long-acting insulin including insulin detemir, insulin glargine (U100, U300), insulin degludec, and PegLispro have shown good evidence for relatively peak-free glucose lowering effect ranging from 18 – 36 hours allowing once-a-day daily basal insulin regimen for most of the patients. However, the need for repeated insulin administration and concurrent risk of nocturnal hypoglycemia are still most feared and costly complications of current therapies. Subsequently, 60% of people with type-1 DM and 45% of people with type-2 DM fail to achieve their target blood glucose levels [8,9]. Improper management of glycemia can lead to life threatening adverse effects owing to the glucotoxic effects on nerves, blood vessels and organs leading to complications of major vascular organs such as heart diseases, high blood pressure, stroke, nephropathy, neuropathy, peripheral artery disease, and reduced quality of life [10,11]. Moreover, day-to-day variability, low patient compliance and progressive micro and macrovascular risks mandate further investigations to formulate long term controlled release basal insulin delivery systems [12].

Polymeric delivery systems have been investigated extensively for controlled release of therapeutics. Copolymers composed of hydrophobic (PLA) and hydrophilic (PEG) blocks have been optimized in multiple studies to obtain diffusion-controlled release tailored to specific needs [13–17]. Subcutaneously injectable *in situ* gel forming delivery systems have also demonstrated prolonged sustained release clinically with good compliance and reproducible release profile [18,19]. Copolymers with varying lengths of hydrophilic (PEG, PGA) and hydrophobic (PLA, PLGA) blocks can be optimized to demonstrate aqueous solubility, amphiphilicity, and phase-transition ability in response to temperature [20]. Moreover, PLA-PEG-PLA based *in situ* gel forming systems have demonstrated ease of formulation, optimization and administration in multiple investigations along with biocompatibility and biodegradability, making them promising candidates for controlled release of basal level insulin [13,14]. In the previous work from our group, we have shown the capability of zinc and chitosan to improve the thermostability and release profile of insulin from poly(D,L-lactide)-poly(ethylene glycol)-poly(D,L-lactide) (PLA-PEG-PLA, 4500 Da) based delivery system. It was observed that chitosan-zinc-insulin complex released insulin at a controlled rate achieving relatively peak-free glycemic control of ~ 63 days in streptozotocin (STZ)-induced type 1 diabetic rats. However, high burst release, higher than normal serum basal insulin concentration (> 40 mU/L) and shorter *in vivo* release compared to *in vitro* were observed which were major limiting factors for clinical progress. Continued investigations with varying chain length of chitosan [11], studying copolymer degradation over time [7,11], and different fatty acid chain length modifications of chitosan (not reported), have been monumental in optimizing the delivery system reported in this study. Examination using varying chain lengths of chitosan showed fast degradation of copolymer matrix with increasing chain length of chitosan (200 kDa, large hydrophilic polymer) implying formation of larger pores during release of large hydrophilic complexes, and slow copolymer degradation with sustained insulin release profile using smaller chain length

chitosan (5 kDa, small hydrophilic polymer). It is well understood that the nature of the incorporated material plays a crucial role in the release characteristics through such copolymeric delivery systems [21]. Additionally, PLA/PEG/PLGA based thermogels attain a domain structure (core-shell) with hydrophilic PEG chains forming the shell of the micelles and hydrophobic PLA chains forming the core of the micelles. Hydrophilic and hydrophobic molecules are assumed to partition between the hydrophilic and hydrophobic domains, where initial release relates to a diffusion-controlled phenomenon from the hydrophilic domain followed by degradation-controlled release from the hydrophobic domain, which has not yet been successfully explored [10]. Moreover, hydrophobic modification of chitosan may also be helpful in improving storage stability of insulin inside the gel depot by excluding water from the proximity of the chitosan-zinc-insulin complexes. Along with this, use of a relevant, clinical-product control (long-acting insulin, glargine) and monitoring diabetes complications frequent with multiple daily administration are essential requirements for preclinical evaluations.

In the present study, we have explored hydrophobic modification of chitosan-zinc-insulin complexes to allow formation of a depot inside the hydrophobic core of the copolymeric micelles thereby promoting dominance of diffusion-controlled release for a prolonged duration and protection from hydrophilic degradation. Depot-in-depot formation further allows for low burst release and slow diffusion from the copolymeric matrix thereby allowing sustained maintenance of physiologically relevant basal insulin release. Stability of insulin was improved by formation of zinc-insulin hexamers. Hexameric form of insulin was further stabilized by electrostatic complex formation with chitosan polymers. Thermal stability and electrostatic complex formation of insulin were studied using nano differential scanning calorimetry (nano DSC) and isothermal calorimetry (ITC), respectively. Conformational and chemical stability of insulin was assessed using circular dichroism spectroscopy (CD) and reversed phase high performance liquid chromatography (RP-HPLC), respectively. Biocompatibility (*in vitro* and *in vivo*) along with immunogenic potential of the insulin released was determined. *In vivo* bioactivity was assessed in STZ-induced type 1 diabetic rat model. Daily administration of insulin glargine (U100), was used as marketed clinical-product control. Efficacy of the delivery system in achieving healthy blood glucose level and preventing complications were assessed by monitoring body weight, blood glucose level, ketone body formation, and cataract formation [22].

2. Materials and methods

2.1. Materials

Human recombinant insulin (Cell Prime™ r-insulin) was obtained from Millipore Corporation (MA, USA). Zinc acetate (anhydrous) was purchased from Alfa Aesar, (MA, USA). Chitosan (5 kDa, ~10% degree of acetylation) was purchased from Glentham Life Sciences (WIL, UK). 1-Ethyl-3-(3-dimethylaminopropyl) carbodiimide hydrochloride (EDC.HCl) was procured from Creosalus Inc. (KY, USA). 2,4,6-Trinitrobenzenesulfonic acid solution (TNBSA) and 3-(4,5-dimethylthiazol-2-yl)-2,5-diphenyl-tetrazolium bromide (MTT) were purchased from Sigma-Aldrich (MO, USA). N-hydroxysuccinimide (NHS) was procured from Alfa Aesar (MA, U.S.A.). Oleic acid was purchased from Spectrum Chemical

(NJ, USA). Streptozotocin was procured from Enzo Life Sciences (NY, USA). MicroBCA protein assay kit was bought from Pierce Biotechnology Inc. (Rockford, IL, USA). Human insulin ELISA kit was purchased from Mercodia (Uppsala, Sweden). Rat Immunoglobulin G (IgG) was obtained from Alpha Diagnostic International (TX, USA). Human embryonic kidney (HEK 293) cell line, Dulbecco's modified Eagle's medium (DMEM) and phosphate buffered saline (PBS) were purchased from American Type Culture Collection (ATCC, Rockville, MD, USA). All other reagents were purchased in analytical grade and used without any modification.

2.2. Synthesis and characterization of oleic acid grafted chitosan polymer

Oleic acid grafted chitosan oligosaccharide polymer (OA-g-CSO) was synthesized using carbodiimide mediated coupling reaction as described in our previous work with slight modifications [23]. Briefly, deionized (DI) water acidified to pH 5.0 using glacial acetic acid was used to dissolve CSO to a final concentration of 50 mg/mL. OA (0.3 or 0.6 mol/mol of free amino group per monomer unit of CSO) was dissolved in 1 mL of ethanol. EDC.HCl (5 mol/mol of oleic acid) and NHS (5 mol/mol of OA) were added to the OA solution followed by stirring on a magnetic stirrer to allow complete mixing. After 20 min, the mixture of activated OA in ethanol was added dropwise to CSO solution under constant stirring. The reaction was continued at 25 °C for 12 h. The resultant product was dialyzed using 1 kDa molecular weight cut off dialysis membrane (Thermo Scientific, IL, U.S.A.) against deionized water for 24 h to remove water soluble by-products, followed by lyophilization to remove water. The freeze-dried product was washed thrice by mixing it with ethanol and filtration through 0.2 μm nylon filter paper. The precipitate was vacuum dried to obtain the OA-g-CSO polymer. OA conjugation on CSO was confirmed using proton nuclear magnetic resonance (^{1}H NMR) and fourier-transform infrared spectroscopy (FT-IR) techniques. Percent conjugation of OA was quantified using trinitrobenzene sulfonic acid (TNBSA) reagent.

For ^{1}H NMR experiments, CSO and OA-g-CSO polymer solutions were prepared in deuterium oxide containing 1% deuterated acetic acid at a concentration of 20 mg/1.2 mL. ^{1}H NMR spectra were recorded using a 400 MHz Bruker spectrometer at 25 °C (32 scans and 1.5 s delay) and analyzed using Bruker TopSpin software (version 3.2.b.69). Thermo Scientific Nicolet iS-10 was used to record the FT-IR spectra of polymer samples. Samples were placed on the diamond crystal iTX accessory and scanned using the parameters set to 0.482 cm^{-1} data spacing, 4.0 resolution, and 64 scans. Background scans were recorded by scanning cleaned diamond crystal accessory before each sample analysis. OMNIC (version 9.3.30, Thermo Scientific) software was used for data analysis following subtraction of background scan from sample scan. Percentage of fatty acid conjugation was determined using TNBSA, a sensitive bio-reagent for quantitative determination of free amine groups. Briefly, 0.2 mg/mL sample solution was prepared in sodium bicarbonate buffer (0.1 M, pH 8.5) in a glass vial. TNBSA reagent (0.02% w/v, 0.25 mL) was added to 0.5 mL of each sample and mixed well. The solution was incubated at 37 °C for 2 hours followed by addition of 0.125 mL of 1N HCl to each sample. Absorbance was measured at 335 nm using a spectrophotometer. Six replicates were performed for each sample. CSO polymer without any grafting was taken as control. Percentage grafting was determined using equation 1.

$$GR\% = (1 - A_{test}/A_{control}) \times 100\% \quad (1)$$

Where, A_{test} is average recorded absorbance of OA-g-CSO polymer and $A_{control}$ is the average recorded absorbance of the CSO polymer without any grafting.

2.3. Calorimetric investigation of insulin modified using zinc and chitosan

2.3.1. Nano differential scanning calorimetry analysis for determining thermal stability—

Thermal transition of insulin before and after preparation of zinc-insulin hexamers and electrostatic complexes with CSO polymer was determined using nano DSC (TA Instruments, USA). Zinc-insulin hexamers were formed by addition of zinc acetate dissolved in 10 mM HCl to insulin solution dissolved in PBS, 10 mM, pH 7.4, at 25 °C with mild shaking for about 10 min. Final molar ratio of zinc ions to hexamer unit of insulin was 1:5 (0.0262 mg zinc acetate per mg of insulin). Electrostatic complex formation between zinc-insulin hexamers (net surface charge: negative) and CSO (net surface charge: positive) was facilitated by adding CSO polymer (5 moles of free amine groups per CSO monomer unit, per mole of hexameric insulin) to zinc-insulin hexamers and allowing incubation at 25 °C for 12 – 15 min with mild mixing. OA-g-CSO-zinc-insulin complexes with different degree of OA grafting (25%, 45%) were prepared in identical manner. Degassed samples were loaded into nano DSC cells. Thermograms were obtained by scanning at a rate of 1 °C/min starting from 10 – 110 °C. Reference scan measured using PBS only was used to measure background interference and deducted from sample scan while analyzing data using Nanoanalyze® software. Amount of different CSO polymers used, calculated based on free amino groups available to form electrostatic complexes with zinc insulin hexamers in 5:1 molar ratio, was considered during data analysis. Transition curve were fitted using two-state scaled model.

2.3.2. Isothermal calorimetry analysis for determining binding interactions—

Effect of hydrophobic modification on CSO polymer, on electrostatic complex formation with zinc-insulin hexamers was determined using isothermal calorimetry technique using nano ITC (TA instruments, USA) thermostated at 25 °C. Enthalpy, binding, and stoichiometry of interaction between zinc-insulin hexamers and OA-g-CSO polymers was studied using zinc-insulin hexamers, 2 mg/mL as titrand in 1 mL cell volume sample cell, and chitosan polymer solution 1.2 mg/mL as titrant in a Hamilton glass syringe. Both samples were prepared in PBS, 10 mM, pH 7.4. Reference cell was filled with PBS only. Titration proceeded as 10 μL injections, at 400 s intervals, into the sample cell while continuous stirring at 250 rpm. Blank titration of polymer solution titrated into PBS alone was used to assess heat of dilution and was subtracted during data analysis to determine net binding heat changes. Data analysis for 25 consecutive injections was performed using Nanoanalyze® software.

2.4. Formulation of delivery systems

Triblock copolymer PLA-PEG-PLA (1500-1500-1500, 4500 Da) was used as the thermogel selected based on promising results from previous studies [14]. Synthesis of copolymer was performed using ring opening polymerization method with reactants D, L lactide and PEG

catalyzed by stannous octoate in nitrogen atmosphere as discussed earlier [24]. Structural composition was determined using ^{1}H and ^{13}C NMR and molecular weight distribution was assessed using gel permeation chromatography (GPC) as previously determined [24]. Phase transition of aqueous copolymer solution from solution to gel to precipitate forms in response to temperature was determined using tube inversion method and has been reported in our earlier studies [24]. Formulations were prepared by mixing insulin, zinc-insulin hexamers, CSO-zinc-insulin complexes or $OA_{(45\%)}$-g-CSO-zinc-insulin complexes, in copolymeric solution (35% w/v in PBS) followed by vortex mixing as described earlier [24]. Briefly, zinc acetate was added to insulin dissolved in PBS to obtain hexameric form of insulin at five molar ratio of zinc ions per insulin hexamer. CSO or $OA_{(45\%)}$-g-CSO-zinc-insulin complexes were prepared by adding CSO polymer to zinc-insulin hexamers at 25 °C for 15 – 20 min with mild intermittent mixing. Amount of CSO polymer added was calculated by molar basis of free amino groups on CSO monomer per mole hexamer at ratio 5:1. Zinc-insulin hexamers, CSO-zinc-insulin or OA-g-CSO-zinc-insulin complexes were collected following centrifugation for 10 min, at 4 °C and 3,000 rpm. The precipitates were homogenously suspended in copolymer solution to obtain the final formulation. Free/non-complexed insulin was quantified in the supernatant using bicinchoninic acid protein assay kit. Phase transition and syringe-ability of the final formulation was confirmed using tube inversion method and injection through a 25G needle, respectively (Figure S1).

2.5. Studying release profile of insulin in vitro

Release profile of different copolymeric formulations was determined in a temperature-controlled water bath set at 37 °C with horizontal agitation of 35 rpm. Comparison of formulation prepared using either free insulin, zinc-insulin hexamers, CSO-zinc-insulin complexes or OA-g-CSO-zinc-insulin complexes was performed. Formulations (0.5 mL) were injected into borosilicate glass tubes (tube length 100 mm, tube length 13 mm, round bottom, with polytetrafluoroethylene rubber-lined screw caps) and incubated at 37 °C water bath to allow phase transition to a gel depot. PBS (5.0 mL, 10 mM, pH 7.4, 37 °C) was added as release medium. Tubes were tightly closed during the study to prevent evaporation of release medium. Samples (1 mL) of release medium were aliquoted at regular intervals from the center of the tube followed by replacement with fresh pre-warmed PBS (1 mL). Insulin released was assayed using bicinchoninic acid protein assay kit and cumulative amount of insulin released over time was calculated following concentration correction [25].

2.6. Stability studies

2.6.1. Analyzing stability of insulin released from delivery system—

Insulin released from optimized formulation *in vitro* was further investigated for thermal stability using nano DSC, chemical stability using RP-HPLC, and conformational stability using CD spectroscopy. Nano DSC was used to check the thermal transition midpoint temperature and enthalpy change of released insulin as mentioned earlier. Chemical stability was determined by RP-HPLC using Agilent 1120 compact LC system using chromatographic conditions presented in table 2. Data acquisition and analysis was performed using EZChrom Elite™ 3.3.2 software (Agilent, CA, USA). CD spectroscopy was used check the tertiary and secondary structural stability by observing the sample spectrum in near-UV region (250 – 300 nm) and far-UV region (200 – 250 nm), respectively. Scans were performed at a rate of

5 nm/min at 20 °C using a 0.1 cm path length quartz cuvette. Fresh PBS scan was subtracted from the sample scan prior to data analysis to remove any background interference. Spectra manager®2 software provided with the instrument was used for analysis of spectrum and secondary structure estimation.

2.6.2. Assessing stability of insulin in formulation during storage—Long-term storage stability of insulin in optimized formulation was also determined. Final formulation samples (1 mL aliquots) were stored in clear borosilicate glass-sample vials, tightly closed and sealed with paraffin film under ambient conditions. Samples were analyzed following 1, 3, 6 and 9 months of storage at 4 °C in a refrigerator. Combination of PBS and acetonitrile (1:1 v/v) was used to extract insulin from stored copolymer formulations followed by analysis using nano-DSC, RP-HPLC and CD spectrophotometer as specified in previous sections.

2.7. Biocompatibility of delivery system

2.7.1. In vitro Biocompatibility—Biocompatibility of the copolymer with and without OA-g-CSO polymer was tested *in vitro* in fibroblast cells (3T3–L1) and human embryonic kidney cells (HEK-293). 3T3–L1 cells were used to mimic cyto-compatibility with the cells populated in the subcutaneous skin layer, and HEK-293 cells were used as a sensitive and robust cell culture model for testing cyto-compatibility of copolymer and its degradation products [13,26]. Copolymer solution (0.5 mL, 35% w/v in PBS) with and without OA-g-CSO was extracted into PBS (10 mM, pH 7.4, 5 mL) following 10-day incubation at 37 °C to mimic accumulation of copolymer degradation products at physiological temperature. Extraction was also performed at 70 °C to mimic long-term accumulation of copolymer degradation products since the degradation rate of PLA/PEG based copolymers is increased at higher temperature. Cells were plated in 96-well plates and allowed to attach. Copolymeric extracts were further diluted using serum-free DMEM followed by incubation with the cells for 24, 48, or 72 hours. Post-incubation, MTT dye was used to quantify the relative cell viability. Untreated cells and cells treated with formalin buffer were taken as negative and positive control, respectively. Relative cell viability was reported and was calculated using following equation 2.

$$\text{Cell viability}(\%) = (A_{\text{treated}}/A_{\text{untreated}}) \times 100 \quad (2)$$

Where, A_{treated} is average recorded absorbance of cells treated with dilutions of polymer extract and $A_{\text{untreated}}$ is the average recorded absorbance of cells in the control wells that were incubated with serum-free DMEM only.

2.7.2. In vivo biocompatibility—*In vivo* biocompatibility of the formulation was evaluated by injecting 0.5 mL of the delivery system or saline subcutaneously in the dorsal neck region of rats. The depot-site was monitored regularly by visual examination. The rats were sacrificed at 1, 7, 30, 90 days' post s.c. administration, followed by excision of the subcutaneous tissue surrounding the injection site and fixing them in 10% neutrally buffered formalin. Histological analysis was performed using tissue sections of 5μm thickness stained with hematoxylin eosin (H&E) and Gomori's trichome stains for visualization of

inflammatory cells and presence of collagen deposition, respectively. Subcutaneous tissue collected from rats without any injection and post-injection with 5% (v/v) neutral buffered formalin were taken as negative and positive controls, respectively.

2.8. In vivo insulin release and bioactivity

Animal study protocol and experiments were reviewed and approved by the North Dakota State University Animal Care Use Committee (IACUC). Male Sprague-Dawley rats weighing 180 – 200 g were used in this study. Rats were housed in a temperature-controlled facility maintained at 12 h light-dark cycle with *ad libitum* access to food and water. At the end of the study rats were euthanized using CO_2 asphyxiation.

2.8.1. Type-1 diabetes induction—After acclimatization to the housing conditions, single dose of STZ (55 mg/kg body weight) prepared fresh each time in ice cold citrate buffer (0.1 M, pH 4.5), was injected intraperitoneally for diabetes induction. Post-injection rats were housed in groups of two per cage and provided with 5% (w/v) sucrose solution in drinking water to counteract the potential risk of hypoglycemia expected by massive insulin release under the influence of STZ. One-week post STZ injection blood glucose levels were measured following 12 h overnight fast. A lancet was used to obtain a drop of blood (< 20 μL) tested using Contour®Next blood glucose meter and glucose testing strips (Ascensia Diabetes Care, NJ, USA). Animals which demonstrated fasting blood glucose levels higher than 200 mg/dL were considered diabetic and were randomly assigned to the treatment groups (Groups II – VII) as described in table 3.

2.8.2. Formulation administration—Assuming basal insulin requirement of 0.5 IU/kg/day, a total dose of 45 IU/kg body weight enough for 90 days was selected for controlled basal insulin release. Rats without any treatment were used as healthy control (Group I). STZ treated diabetic rats without any insulin treatment were taken as negative control (Group II). Group III was injected s.c. with a single dose of insulin solution (0.5 IU/kg) dissolved in PBS (10mM, pH 7.4). Group IV was injected s.c. with once-daily glargine (Lantus® U-100) at a dose of 0.5 IU/kg/day for 90 days. Group V – VII were injected s.c. with a single dose of copolymeric formulation incorporating either free insulin, CSO-zinc-insulin complexes or OA-g-CSO-zinc-insulin complexes, injected s.c. at the dorsal neck region using a 25 G needle (Table 3).

2.8.3. Blood sampling and quantification of serum insulin level—Blood sampling was performed on overnight fasted rats using tail vein puncture. Blood samples were allowed to coagulate for 30 min at room temperature and serum was collected following centrifugation at 2000 g for 10 min at 4 °C. Insulin was quantified using human insulin enzyme linked immunosorbent assay (Mercodia Human Insulin ELISA (Uppsala, Sweden) Catalog# 10-1113-01) using manufacturer's protocol.

2.8.4. Determination of blood glucose and ketone levels—Blood glucose levels were measured 12 h overnight fasting using Contour®Next blood glucose meter and glucose testing strips. Blood ketone levels were measured similarly at 1, 2, and 3-month interval

analyzed using Precision Xtra® blood ketone meter and ketone testing strips (Abott Diabetes care, CA, USA).

2.8.5. Determination of cataract formation—Cataract formation in rats was determined visually and considered partial for strong nuclear cataract formation with perinuclear area opacity (< 75%), and complete for total opacity of lens [27,28].

2.8.6. Determination of body weight—Body weight of the animals before and after STZ-treatment and following insulin treatment was noted regularly over the entire study duration.

2.8.7. Detection of anti-insulin antibodies—Rat serum samples collected after 1, 2 and 3 months after treatment were analyzed for rat anti-insulin IgG antibodies using indirect ELISA (Alpha Diagnostic International (TX, USA), Catalog# 3750-RIG) using manufacturer's protocol.

2.9. Statistical analysis

Data obtained are presented as mean ± SD. Statistical analyses were performed using two-tailed unpaired student's t-test and one-way ANOVA with post-hoc Tukey HSD test using GraphPad Prism software (version 5.01). A p value of less than 0.05 was considered to be significant. For sound statistical analysis of the results, six animals will be used for each group for *in vivo* studies. G*Power 3.1.9.2 calculation was performed considering small effect size, 0.05 α error, and 0.8 test power.

Results and discussion

3.1. Synthesis and characterization of oleic acid grafted chitosan polymer

In our previous work, chain length of chitosan was found to play a crucial role in controlling the overall size of chitosan-zinc-insulin complexes, formation of holes and tunnels in the copolymer matrix during initial release, thereby affecting the subsequent release of therapeutic (insulin) through the thermogel delivery system [24]. Chitosan chain length 5 kDa was found to be optimum and was selected for further investigation. OA-g-CSO polymer was successfully synthesized using carbodiimide mediated coupling reaction. In this reaction 1-ethyl-3-(−3-dimethylaminopropyl) carbodiimide hydrochloride (EDC.HCl) along with N-hydroxysuccinimide (NHS) create a highly reactive intermediate upon interaction with the carboxyl group of fatty acid. The intermediate acylisourea ester then reacts with primary amine group of CSO to form peptidyl bond with the elimination of a water molecule. OA grafting on CSO backbone was characterized using ^{1}H NMR and FT-IR spectroscopy as shown in figure S2 and figure S3, respectively. ^{1}H NMR spectra of both CSO and OA-g-CSO polymers showed resonance corresponding to N-acetylglucosamine, glucosamine residue, ring protons at 1.9, 3.0, and 3.4 – 3.8 ppm, respectively. Additionally, OA-g-CSO polymer showed peaks corresponding to methyl ($-CH_3$) and methylene ($-CH_2-$) groups of OA residue at 0.8 – 1.1 ppm, and amide bond associated methylene protons at 2.5 ppm. FT-IR spectra of both CSO and OA-g-CSO polymers showed absorption peaks at 1655 cm-1, 1585 cm^{-1} and 1470 cm^{-1} which can be correlated stretching of carbonyl moiety on

secondary amides, N-H bending vibrations of non-acylated primary amines of CSO, and N-H bending vibrations secondary amide band, respectively. OA-g-CSO polymers demonstrated absorption peaks at 2850 – 2950 cm^{-1} which can be suggested owing to the presence of methylene groups on OA. Moreover, with increased grafting percentage absorption intensity of peak at 1470 cm^{-1} decreased while at 1655 cm^{-1} and 1585 cm^{-1}, were found to be increased. Grafting efficiency of OA onto CSO backbone was determine using TNBSA bio-reagent. TNBSA reacts with primary amine groups to form a highly chromogenic derivative (N-trinitrophenylamine) which can be quantified using absorption spectroscopy [29,30]. OA-g-CSO polymers with 25 ± 0.2 % and 45 ± 0.5 % grafting percentage were selected for further characterization in this study.

3.2. Calorimetric investigation of insulin modified with zinc and chitosan

Effect of addition of zinc, CSO and OA-g-CSO polymers on the association state and thermal stability of insulin were investigated using nano DSC. Transition midpoint temperature (Tm) and transition enthalpy (ΔH) was determined for respective association state of insulin as summarized in table 4. The DSC thermogram obtained shows transition of free insulin monomers at Tm_1 51.87 ± 0.23 °C and insulin dimers at Tm_2 62.81 ± 0.29 °C (Figure 1) [31,32]. Addition of zinc ions allows association of three insulin dimers to form zinc-insulin hexamer with significantly improved thermal stability indicated by a higher Tm value of 72.57 ± 0.19 °C. Neutron crystallographic analysis suggests zinc-insulin hexamers have a net negative charge at physiological pH [33]. CSO polymer, which is positively charged at physiological pH, stabilizes the hexameric form of insulin by forming electrostatic complex with negatively charged zinc-insulin hexamers resulting in significantly improved thermal stability of insulin as indicated by higher Tm value ~ 86 °C. OA modification of CSO demonstrated lower Tm and ΔH values indicating somewhat lower thermal stability of insulin upon complexation with OA-grafted-CSO compared to CSO polymer. This could be attributed to reduced positive charge on CSO backbone and weaker electrostatic complex formation between OA-g-CSO and zinc-insulin hexamers. The complex formation between OA modified CSO polymers and zinc-insulin hexamers was further studied using ITC.

Isothermal analysis was performed to quantitatively determine binding affinity between zinc-insulin hexamers and hydrophobically modified CSO. Integrated net binding heat changes obtained using different grafting ratio of OA onto CSO polymer interacting with zinc-insulin hexamers is shown in figure 2. Electrostatic interaction between CSO polymer and zinc-insulin hexamer results in an exothermic reaction. Each subsequent injection of CSO polymer into the sample cell resulted in interaction with zinc-insulin hexamers neutralizing the negative charge indicated by reduced heat changes. Thermodynamic parameters of the respective interactions are summarized in table 5. The ITC thermogram for unmodified CSO titrated into zinc-insulin hexamers corresponded to higher binding constant (k) and more exothermic heat changes (ΔH) compared to OA-g-CSO polymers, indicating high binding affinity and stronger electrostatic complex formation between CSO and zinc-insulin hexamers. This effect was well correlated to that observed using nano-DSC demonstrating higher transition enthalpy for CSO-zinc-insulin complexes (Table 4). This effect may be explained by reduced number of free amino groups upon OA grafting on CSO

resulting in weaker ionic interaction between OA-g-CSO polymer and zinc-insulin hexamers. Free CSO polymer forms stronger electrostatic complex owing to higher positive charge density compared to OA-modified CSO polymer. Furthermore, increase in OA substitution may lead to reduced value of binding constant and enthalpy of complex formation which may result in comparatively lower temperature-associated stability of insulin. Hence, OA modification of CSO can have detrimental effect on electrostatic complexes formed between CSO and zinc-insulin hexamers which may ultimately play a crucial role in the overall stability and release of insulin from such complexes. However, OA grafting up to 45% showed comparable binding affinity to unmodified CSO indicating stable electrostatic interactions between OA-g-CSO polymer and zinc-insulin hexamers, which would play an essential role in maintaining insulin in a stable form throughout the duration of release and storage.

3.3. Studying release profile of insulin in vitro

Cumulative release profile of insulin, zinc-insulin hexamers, CSO-zinc-insulin complexes and $OA_{(45\%)}$-g-CSO-zinc-insulin complexes incorporated in thermosensitive copolymer solution is shown in figure 3. Free insulin incorporated in thermogel copolymer demonstrated a high early burst release (15.2 ± 2.2%) owing to the immediate release of hydrophilic insulin molecules present at the surface of the copolymeric depot. Formation of zinc-insulin hexamers and CSO-zinc-insulin complexes significantly reduced initial burst release to 10.1 ± 1.3% and 5.1 ± 0.7% respectively, compared to free insulin, from their respective thermosensitive copolymeric delivery systems. This was observed due to the slow movement of larger zinc-insulin hexamers and CSO-zinc-insulin complexes through the copolymer depot. Hexamer formation with zinc reduces overall hydrophilicity of the incorporated insulin reducing burst release, restricting diffusion and controlling the rate of release of insulin from the copolymeric depot for ~ 49 days in comparison to free insulin which shows release up to 28 days. Both free insulin and zinc-insulin hexamers containing formulation demonstrated a secondary burst release at 14 and 28 days, respectively. This is observed due to the faster release of incorporated insulin upon breakdown of the PLA chains. However, addition of CSO to the copolymeric depot minimizes secondary burst release and demonstrates constant release of insulin at a sustained rate for up to 70 days. This phenomenon is attributed to the buffering action of CSO polymer which resists pH change in its microenvironment, helping in reducing degradation rate of the copolymer and resulting in extended insulin release for a longer duration [23]. OA-g-CSO-zinc-insulin complexes further extended the rate of insulin release up to 80 days. As mentioned earlier, PLA-PEG-PLA copolymer would attain a domain structure with a hydrophobic core and hydrophilic shell [34]. Hydrophobic modification of insulin by preparing OA-g-CSO-zinc-insulin complexes allows for its incorporation into the hydrophobic domain of PLA-PEG-PLA copolymer micelles. This results in slow diffusion of incorporated complexes throughout the degradation dominant stage resulting in significantly reduced burst release of insulin (3.8 ± 1.7%) followed by sustained release profile for a prolonged period. Slow diffusion of insulin combined with buffering action of CSO polymer can together help achieve zero-order release profile of insulin relevant for providing physiological basal insulin needs.

3.4. Stability studies

3.4.1. Analyzing stability of insulin released from delivery system—Structural and conformational stability of insulin is pertinent to its biological activity. Insulin is a small globular protein that is present in nature in different oligomeric forms, mainly monomers, dimers, and hexamers. Insulin in its monomeric form is susceptible to denaturation and fibril formation while dimers and hexamers are more stable. Therefore, stabilization of insulin hexameric structure is an effective means of improving insulin stability and counteracting fibril formation [35]. Conformationally, insulin comprises of higher order structures and alteration in its primary, secondary, tertiary or quaternary structure greatly influences its biological activity [36,37]. Therefore, controlled delivery systems intended for prolonged use of protein/peptide based therapeutics must ensure structural and conformational stability as well as prevention of denaturation and aggregation of cargo protein [37,38]. Increasing the chain length of hydrophobic PLA block in PLA-PEG-PLA triblock copolymer allows for lower water content in the gel [34]. This further protects the incorporated insulin from degradation and/or aggregation inside the depot. CD spectrum recorded in the near UV region (250 – 300 nm) measures differential absorption of left and right circularly polarized light by aromatic amino acid side chains (phenylalanine, tryptophan, tyrosine) providing an estimate of tertiary structure of a protein [39]. Fresh insulin sample scan demonstrated a peak at ~ 273 nm depicting stable tertiary structure of insulin (Figure 4A). Spectrum obtained by scanning insulin samples released up to 90 days showed strong CD signal ~ 273 nm representing stable tertiary structure of insulin. Presence of secondary structural components (α helix, β sheets, and random coils) determined using CD can be used to evaluate conformational stability of proteins/peptides including insulin [14,40–42].

CD spectrum in the far UV region (200 – 250 nm) provides an estimation of secondary structural features of insulin [39]. Scanning freshly prepared insulin solution in the far UV region demonstrates two minima at ~ 208 and 225 nm indicating presence of α helices (34.6 ± 1.7 %) and β sheets (4.8 ± 3.3 %) (Table S1). Insulin released from copolymeric depot demonstrated strong peaks at 208 and 225 nm confirming the ability of OA-g-CSO-zinc-insulin complexes in preserving conformational stability of insulin during the overall period of release (Figure 4B). *In vitro* assessment of thermal stability of insulin can be performed using nano-DSC, such as determination of association state and folding/unfolding temperature. DSC thermogram of samples of insulin released *in vitro* from OA-g-CSO-zinc-insulin complexes incorporated in thermosensitive copolymer depot demonstrated Tm values corresponding to the transition of OA-g-CSO-zinc-insulin complexes at initial time points, which later dissociated to zinc-insulin hexamers upon dilution (Figure 4C). High Tm values indicate prevention of aggregation of zinc-insulin hexamers in the depot when complexed with OA-g-CSO, allowing it to be released in a stable form for up to 90 days [13,14,43,44]. Furthermore, detection of proteins and peptides and their degradation/aggregation products using RP-HPLC, is an effective tool for assessing their chemical stability. RP-HPLC is a versatile and reliable technique that enables detection of both covalent and non-covalent aggregates at low concentration based on their affinities towards a n-alkyl silica-based stationary phase, and an organic solvent mobile phase (e.g. acetonitrile) containing a strong ion-pairing agent (e.g. trifluoroacetic acid, TFA) to improve retention in the column. In this study, analysis of insulin released at 1, 30, 60 and 90 days using RP-HPLC showed retention

of stable insulin ~ 11.6 min comparable to retention of freshly prepared insulin solution (standard) (Figure 4D). Moreover, in our previous studies Native-PAGE, SDS-PAGE and MALDI-TOF MS analyses have been performed to demonstrate stability of insulin and identification of its degradation products following release from PLA-PEG-PLA (1500-1500-1500, 4500 Da) polymeric formulations and inside the gel during storage and release [43].

3.4.2. Assessing stability of insulin in formulation during storage—

Depot-in-depot formation of OA-g-CSO-zinc-insulin complexes in PLA-PEG-PLA copolymer micelles reduces their interaction with the hydrophilic domain allowing for improved stability and shelf-life of such delivery systems [45,46]. Additionally, positively charged OA-g-CSO polymer forms electrostatic complex with negatively charged zinc-insulin hexamers and stabilizes the insulin in hexameric form further improving its stability [14,42]. Insulin extracted from stored copolymer formulations showed stable tertiary and secondary structure in the near and far-UV region of CD spectrum after 1, 3, 6 and 9 months of storage at 4 °C (Figure 5A and 5B). Nano-DSC and RP-HPLC of the extracted insulin samples also demonstrated the presence of insulin in stable form as compared to freshly prepared standards up to 1, 3, 6, and 9 months' post storage at 4 °C (Figure 5C and 5D). These analyses demonstrate the exceptional ability of PLA-PEG-PLA copolymer and complex formation with CSO in preserving the structural and conformational stability of insulin in the prepared formulation for storage up to 9 months in refrigerated conditions.

3.5. In vitro and in vivo biocompatibility

This study was designed to evaluate the effect of short and long-term accumulation of PLA-PEG-PLA triblock copolymer with and without OA-g-CSO polymer by determining the effect of their degradation products on 3T3–L1 fibroblast cells and HEK 293 cells. Although copolymers constituting PLA and PEG are widely researched to be biodegradable and biocompatible, their long-term accumulation at the depot site needs to be investigated to demonstrate their safety for prolonged and/or repeated use [47–49]. OA-g-CSO polymer was also added to aqueous copolymer formulation while assessing the biocompatibility of the delivery system. Insulin and zinc were not included in this study owing to their effect on cellular properties such as cell proliferation which may interfere with distinctly assessing cytotoxic effects of the copolymeric delivery system [50,51]. In this study, both 3T3–L1 and HEK-293 cells showed good cytocompatibility post incubation with copolymer extracts with and without OA-g-CSO polymer (Figure 6). It was noted that the presence of OA-g-CSO polymer improved cell viability, which can be associated with the cell proliferative and wound healing properties of CSO [52]. Longer incubation period up to 48 and 72 h as well as extraction of copolymer at higher temperature (70 °C), both resulted in increased viability in both cell types indicating the positive contribution of copolymer degradation products in cell proliferation and viability. This is suspected to occur due to the consumption of copolymer degradation products *via* citric acid cycle leading to higher mitochondrial activity and cellular metabolism [53]. However, *in vivo* biocompatibility is a much more complex phenomenon. Various natural, synthetic and semisynthetic materials have been used for manufacturing implantable devices [54]. The major concern following such implantation is

foreign body response resulting from the tissue injury due to implantation along with the continued presence of the implant in the region.

PLA-PEG-PLA based copolymers have an added advantage of being easily injectable, formation of *in situ* depot at injection site, and aqueous solubility avoiding the use of harmful organic solvents which can damage the incorporated drug substance as well as cause pain/irritation upon administration. The presence of PEG chains forms an outer corona on these copolymeric micelles contributing to their low immunogenicity [55]. Additionally, PLA-PEG-PLA triblock copolymers show simulated mucin like action (mucomimetic characteristics) along with pliability which helps in reduced mechanical irritation from such thermogel depots [56,57]. Treatment of a chronic disease like type-1 diabetes requires all components of the delivery system intended for treatment to be biocompatible for long-term use. To determine the biocompatibility of the PLA-PEG-PLA copolymer incorporating OA-g-CSO-zinc-insulin complexes *in vivo*, the depot was regularly observed and the subcutaneous tissue surrounding the injection site was excised and analyzed for inflammatory response. The chief stages of this process include short lived (few days) acute inflammation, which is mainly an attempt by the body to clear the foreign substance using hemodynamic forces like vascular dilation providing excess blood flow to the site, formation of a fibrin clot, permeation of salts, protein and water to cause edema, and infiltration and accumulation of numerous blood and tissue proteins including cytokines, growth factors and leukocytes. The tissue samples collected 1-day post administration show increased accumulation of inflammatory mediators (Figure 7G). This accumulation is similar to that observed in the control group injected with same volume of saline (0.5 mL) (Figure 7C). Positive control group injected with 5% (v/v) of formalin buffer shows much higher accumulation of inflammatory factors due to the relatively higher irritation and activation of foreign body response (Figure 7B). Continued inflammatory stimuli results in a chronic inflammatory response which proceeds by restructuring of the injection area by proliferation of blood vessels, connective tissue, fibroblasts and endothelial cells leading to conversion of initially formed fibrin clot to a highly vascularized granulation tissue, surrounding the implant. However, in the tissue excised 7-day post administration no such formation was observed in the tissue surrounding the implant (Figure 7H). Eventually active fibroblasts produce collagen and proteoglycans replacing the granulation tissue with extracellular matrix. Well defined collagen fibers form a fibrous wall around the implanted device and confines it from entering the surrounding tissue. Gomori's trichrome stain was used to determine the nature and presence of collagen deposition at the administration site. In our experiments, it was noted that the collagen deposition at the site of injection was increased initially (day 30), indicated by high intensity of stained collagen fibers (Figure 7L). However, the collagen density at the end of the study was comparable to control, with no sign of residual scar tissue. The connective and muscular tissues surrounding the injection site appeared to be normal with no morphological changes compared to control, thus confirming the biodegradable and biocompatible nature of the delivery system.

3.6. In vivo insulin release and bioactivity

The overall aim for insulin therapy is to improve pharmacokinetic (PK) profile to obtain pharmacodynamic (PD) effects closely resembling insulin release and action in a healthy

body [58,59]. Basal insulin release is estimated to be 0.1 – 0.2 U/kg/day in healthy individuals corresponding to fasting insulin concentration < 25 mU/L [2]. Ideal requirements of basal insulin therapy include flat PD profile, low hypoglycemic risk, and stable duration of action. Unfortunately, current insulin options do not fulfill these essential criteria. Insulin NPH (NPH: neutral protamine Hagedom) shows delayed absorption with an onset of 1 – 4 h and peak in 6 – 10 h, suggested as twice daily administration for basal insulin therapy, however high inter-individual variability, short duration of activity, and risk for severe hypoglycemia persuaded the need to develop longer-acting insulin analogues [60]. Insulin glargine is an bioengineered insulin analogue prescribed as once-daily administration to cover basal insulin for a 24 h period. Glargine forms precipitates in the surrounding subcutaneous tissue after injection which slowly re-dissolve delaying the absorption. However, it fails to mimic physiological insulin secretion and require high doses to provide 24 h coverage. High variability in the PK profile in current therapy directly influences PD effects, increasing hypoglycemic incidents due to unpredictability of insulin peaks, fluctuating blood glucose levels and increased occurrence of diabetes complications [61–63]. In an attempt to obtain a peak-less PK profile and reducing the frequency of administration for basal insulin therapy thermosensitive *in situ* gel forming systems have a competitive advantage. Insulin can easily be suspended in aqueous thermosensitive copolymer solution owing to their low critical solution temperature (LCST > 25 °C), which upon subcutaneous administration due to the physiological temperature (35 – 37 °C) being above their upper critical solution temperature (UCST) undergo phase transition to form a gel depot.

As mentioned earlier, these copolymers are biocompatible, biodegradable, and help preserve the stability of insulin inside the depot for the entire duration of release and storage. However, for modifying this system for basal insulin delivery three critical parameters *i.e.* burst release, release profile of insulin, and bioactivity of insulin released need to be considered. The initial burst release occurs due to the rapid release of therapeutic present on the surface of the depot. Burst release of insulin from such delivery systems needs to be addressed to avoid hypoglycemia. Thereafter, the release of therapeutic is dependent on diffusion through the copolymer matrix at an early stage followed by a combination of diffusion through the copolymer and degradation of copolymer at later stage [64]. Reduction in peaks and troughs throughout the duration of release is beneficial in mimicking physiological insulin release. In this study, we compared the PK profile of three thermosensitive copolymer-based formulations (Groups V, VI and VII) incorporating free insulin, zinc-insulin hexamers and OA-g-CSO zinc insulin complexes, respectively, with free insulin solution (single administration) and insulin glargine solution (Lantus® U-100, repeated administration at 24 h interval) (Table 3). Insulin solution resulted in C_{max} of 61.74 ± 6.47 mU/L with T_{max} 2 h followed by immediate absorption and drop in blood glucose with its glucose lowering effect lasting for 6 – 8 h (Figure 8A). Insulin glargine showed a relatively sustained profile of insulin release reaching peak serum concentration between 2 – 4 h and blood glucose lowering effect lasting between 18 – 20 h (Figure 8B). Thermosensitive copolymer formulation incorporating free insulin showed a burst release of 58.13 ± 5.01 mU/L in 24 h, followed by slow controlled release for 7 days and complete release by ~ 35 days (Figure 9). Both CSO-g-zinc-insulin complexes and OA-g-CSO zinc

insulin complexes helped reduce the burst release by ~ 4.8 fold and showed gradual increase in serum insulin levels post administration with 19.95 ± 10.88 and 12.67 ± 4.07 mU/L in 24 h, respectively.

Formulation incorporating OA-g-CSO-zinc-insulin complexes demonstrated relatively stable serum insulin levels of 21.83 ± 3.29 mU/L for ~ 91 days. Formulations incorporating free insulin and CSO-zinc-insulin complexes released insulin at a faster rate demonstrating serum insulin levels of 19 – 65 mU/L over 28 days, and 15 – 42 mU/L over ~ 63 days, respectively. Since the release from such thermogels is significantly affected by the nature and size of the incorporated therapeutic, depot in depot formation by hydrophobic modification CSO polymer contributed significantly to a sustained release profile of insulin for an extended period [24]. Absorption of insulin is a complex phenomenon [65,66]. Association state of insulin has been regarded as the major determinant for its rate of absorption. Biological activity of insulin is manifested by binding of the monomeric form of insulin to the insulin receptor [67]. However, at micromolar concentration insulin monomers self-associate to form dimers. In the presence of zinc, three insulin dimers arrange to form a hexameric complex with reduced solubility. At physiological pH, positively charged CSO polymer (CSO pKa 6.2 – 7) are capable of forming electrostatic complexes with negatively charged zinc-insulin hexamers (insulin pKa ~ 5.3) stabilizing the hexameric complex and preventing aggregation and degradation [68,69]. The complexes upon release undergo dissociation upon dilution to release zinc-insulin hexamers, that dissociate into dimers and finally release insulin monomers that are absorbed into systemic circulation. Slow dissociation of insulin from the complex helps in controlled availability of insulin as well as preserves the conformational and biological stability of insulin up till its release and absorption. Insulin mediates its PD effects through the insulin receptor. This effect was evaluated by monitoring blood glucose concentration in treated rats. High burst release of insulin in diabetic rats treated with insulin solution, and free insulin incorporated in thermosensitive copolymer solution rendered rapid lowering of blood glucose levels from ~ 400 to 72 and 68 mg/dL 2 h post administration, respectively (Figure 8A and 9). This is a serious concern and often requires immediate medical attention as glucose concentrations lower than 60 mg/dL may lead to unconsciousness, seizures, diabetic coma or even death. The rats were duly monitored throughout the duration of blood glucose concentration lower than 75 mg/dL but no severe behavioral symptoms like shakiness, seizures, or abnormal activity were noted. This could potentially be attributed to the coprophagic behavior of rats which may have prevented development of hypoglycemic shock state [14,70,71]. CSO-zinc-insulin complexes and OA-g-CSO-zinc-insulin complexes incorporating formulations resulted in gradual lowering of blood glucose levels of 84 and 104 mg/dL 2 h post administration, respectively (Figure 9). Daily 24 h administration of glargine resulted in fluctuating blood glucose levels between 91 – 443 mg/dL. On the other hand, CSO-zinc-insulin complexes containing formulation resulted in blood glucose levels 97 ± 16 mg/dL for 77 days and OA-g-CSO-zinc-insulin complexes incorporating formulation resulted in blood glucose levels 102 ± 9 mg/dL for 91 days. There was no significant difference ($P < 0.05$) between the blood glucose levels of OA-g-CSO-zinc-insulin complexes formulation group between consecutive time intervals, and with healthy non-diabetic rats up to 63 days which can be attributed to the slow release of insulin diffusing from the depot inside the

hydrophobic depot of the copolymer micelles. Such release profile is extremely beneficial for basal insulin therapy in diabetic individuals as it would prevent hyper- and hypo-glycemic episodes, night-time hypoglycemia, and steady glucose supply in fasting conditions for optimum physiological health and energy production. Moreover, hydrophobic modification of CSO-zinc-insulin complexes also helped achieve better *in vitro - in vivo* correlation which may be beneficial in tailoring the system to basal insulin range between 0.5 – 1 U/h/kg for patient-based therapy.

3.7. Determination of body weight

Treatment of young adult rats with STZ produces a diabetic state characterized by reduced body weight, polyuria, polydipsia and hyperglycemia [72]. STZ preferentially accumulates in pancreatic beta-cells owing to the presence of glucose moiety in its chemical structure allowing selective uptake via the GLUT-2 glucose transporter [73]. STZ then leads to DNA alkylation, fragmentation and damage by supposedly the nitric oxide donor effect of nitrosourea moiety which is cytotoxic thereby destroying beta-cells in pancreas [74]. Sudden weight loss due to diabetes is a common clinical manifestation owing to insufficient insulin production in the body preventing utilization of glucose for cellular energy production. The body then starts burning fat and muscle cells for energy that causes reduction in overall body weight. In all groups treated with STZ, drastic reduction in body weight was observed. However, a gradual recovery in body weight was observed following insulin therapy. Continuous reduction in body weight was observed in untreated (Group II) and insulin solution treated groups (Group III) up to 63 days (Figure 10). Thermosensitive copolymer formulation treated groups demonstrated significant increase in body weight compared to untreated diabetic rats ($P < 0.01$) up to 16 weeks (112 days) post treatment. This can be attributed to the PD manifestation of administered insulin in glucose utilization, maintenance of overall health and energy balance.

3.8. Determination of blood ketone levels and cataract formation

Persistent blood sugar spikes as expected from repeated insulin administration can cause severe complications like diabetic ketoacidocis (DKA), hyperglycemic hyperosmolar syndrome (HHS), damage to blood vessels, nerves, and organs leading to heart disease, stroke, nephropathy, neuropathy, retinopathy, skin infections, limb amputations, problems with teeth and gums, all leading to reduced quality of life and high medical cost. DKA is a life-threatening complication of diabetes which occurs due to build-up of ketones in the body as a result of fat breakdown during insulin-glucose imbalance. In the absence of sufficient insulin, DKA may develop in less than 24 h. In diabetes patients, DKA can be suspected with blood pH < 7.3 and plasma ketone concentration of > 3.0 mmol/L [72]. Inefficient insulin in the body may also cause HHS due to build-up of glucose resulting in high osmolarity, dehydration, and vision problems. This may lead to osmotic lens swelling and cataract development over time. Evaluation of efficient basal insulin therapy mandates prevention of both short and long-term complications of diabetes. Determination of blood ketone levels is an effective strategy of monitoring accumulation of ketones in the body and preventing DKA. STZ-treated diabetic rats (Group II) showed significant accumulation of blood ketones ($P < 0.05$) compared to healthy control with a concentration of 3.8 ± 0.2 and 4.1 ± 0.4 mmol/L within one- and three-months' post STZ-treatment, respectively (Figure

11A). Gradual rise in blood ketone levels was observed in the free insulin and CSO-zinc-insulin complexes incorporated in thermogel copolymer formulations group at two and three-month time-points, respectively. However, owing to the sustained maintenance of basal insulin levels in the OA-g-CSO-zinc-insulin complexes incorporated in thermogel copolymer formulation group there was insignificant build of ketones in the body, suggesting much lower risk of DKA associated complications (Figure 11A).

Daily treatments with insulin-glargine also helped prevent accumulation of ketone bodies, however required timely doses of insulin for 3 months accounting to 90 injections. Visual impairment and cataract development is also a common complication of diabetes. Reduction of glucose to sorbitol occurs through the polyol pathway catalyzed by the enzyme aldose reductase (AR). Hyperglycemia promotes AR-mediated accumulation of sorbitol in lens fibers and increase in osmotic, oxidative and ER stress, along with glycation of lens proteins that lead to degeneration, collapse, and liquefaction of lens fibers, resulting in formation of lens opacities and progression to cataract [72]. All the animals in the diabetic untreated group developed total opacity of lens (Figure 11C). Partial to complete cataract development was observed in insulin solution and free insulin incorporated in copolymer formulation within 60 – 90 days' post treatment (Table 6). However, no sign of cataract development (clear eye lens) was observed in the group treated with OA-g-CSO-zin-insulin complexes containing thermosensitive copolymeric depot-based formulation (Figure 11B). This study emphasizes the importance of steady basal insulin levels in maintenance of metabolic balance, normal physiological functions, and thereby prevention of complications in type-1 diabetes.

3.9. Detection of anti-insulin antibodies

Several protein-based therapeutics have an associated risk of eliciting undesirable immune response in patients that may often lead to reduction in therapeutic efficacy, serious anaphylaxis reaction, or life-threatening auto-immunity. Exogenous insulin preparations continue to be immunogenic to humans, and origin, storage condition, formulation, excipients, association state, aggregation and degradation products, have been discussed to be some of the factors contributing to enhanced immunogenicity [75,76].

In this study OA-g-CSO-zinc-insulin complexes were prepared and incorporated in thermosensitive copolymer solution for sustained release of basal level insulin. Hexameric association state of insulin was stabilized by electrostatic complex formation with OA-g-CSO polymer and maintained in the copolymeric micelles, which slowly diffused out through the copolymeric matrix and dissociated to zinc-insulin hexamers, insulin dimers, and ultimately monomeric insulin to be absorbed in the systemic circulation. To estimate immunogenicity of insulin released from this formulation *in vivo*, presence of anti-insulin antibodies was determined in rat serum samples 1, 2, and 3-months post formulation administration (Figure 11D). Indirect sandwich ELISA technique was employed, and rat IgG antibody was used as positive control. No anti-insulin antibody formation was detected in any of the formulation groups initially as well as up to 90 days after formulation administration. The antibody response after insulin treatment was comparable to untreated control group (Group II). Therefore, it can be safely concluded that the thermosensitive

copolymer-based formulations optimized in this study did not generate any undesirable immune response and the insulin released was non-immunogenic in nature.

3. Conclusion

In this study, we successfully optimized an *in situ* gel forming thermosensitive copolymer-based delivery system that delivers basal level insulin with relatively peak-free pharmacokinetic profile for up to 90 days in type-1 diabetic rat model. Preparation and optimization of oleic acid-grafted-chitosan-zinc insulin complexes helped in localization of insulin in the hydrophobic core of poly-lactide micelles resulting in slow-controlled release of insulin for an extended period while preserving structural, conformational and biological stability of insulin. This system closely mimics physiological basal insulin secretion required to maintain normal glycemic control in type-1 diabetes patients. Moreover, long-term controlled release of basal level insulin may help improve patient compliance while reducing overall economic cost of diabetes by preventing development of diabetes complications.

Controlled release of hydrophilic molecules with short half-life is often a challenging task. However, exploiting simple physiochemical techniques (such as electrostatic interaction with a hydrophobically modified polymer) may contribute to a significant improvement over conventional strategies as observed in our study. Besides, improved thermal stability of insulin upon modification with zinc and chitosan can also be exploited for oral delivery of insulin prior to encapsulation in biocompatible polymeric delivery systems such as PLGA microspheres. Furthermore, PLA-PEG-PLA based thermosensitive copolymeric delivery system explored in this study can also be used for sustained delivery of various other therapeutic proteins and peptides (salmon calcitonin, erythropoietin, monoclonal antibodies, etc.) which require frequent administration over prolonged duration [12].

Supplementary Material

Refer to Web version on PubMed Central for supplementary material.

Acknowledgments

This research was supported by the National Institutes of Health (NIH) grant# R15GM114701.

Abbreviations

DM	diabetes mellitus
PLA	poly(lactic acid)
PEG	poly(ethylene glycol)
CSO	chitosan oligosaccharide
OA	oleic acid
MTT	3-(4,5-dimethylthiazol-2-yl)-2,5-diphenyl-tetrazolium bromide

RP-HPLC	reversed phase high performance liquid chromatography
DSC	differential scanning calorimetry
ITC	isothermal calorimetry
CD	circular dichroism
UV	ultraviolet
Tm	Midpoint transition temperature
ΔH	transition enthalpy
HEK 293	human embryonic kidney cell line
^{1}H NMR	proton nuclear magnetic resonance
FT-IR	Fourier-transform infrared spectroscopy
TNBSA	2,4,6-trinitrobenzene sulfonic acid
GPC	gel permeation chromatography
TFA	trifluoroacetic acid
PDI	polydispersity index
PBS	phosphate buffer saline
DMEM	Dulbecco's modified Eagle's medium
IgG	Immunoglobulin G
ELISA	enzyme linked immunosorbent assay
STZ	Streptozotocin (2-deoxy-2-(3-(methyl-3-nitrosoureido)-D-glucopyranose)

References

[1]. Wilcox G, Insulin and insulin resistance., Clin. Biochem. Rev 26 (2005) 19–39. http://www.ncbi.nlm.nih.gov/pubmed/16278749 (accessed September 17, 2019). [PubMed: 16278749]

[2]. Melmed S, Polonsky KS, Larsen PR, Kronenberg H, Williams textbook of endocrinology, 2015.

[3]. Coelho JFJ, Ferreira P, Gil MH, New approaches in drug delivery systems: application for diabetes treatment., Infect. Disord. Drug Targets 8 (2008) 119–28. http://www.ncbi.nlm.nih.gov/pubmed/18537707 (accessed September 17, 2019). [PubMed: 18537707]

[4]. Porcellati F, Lucidi P, Bolli GB, Fanelli CG, Thirty Years of Research on the Dawn Phenomenon: Lessons to Optimize Blood Glucose Control in Diabetes, Diabetes Care. 36 (2013) 3860–3862. 10.2337/DC13-2088. [PubMed: 24265365]

[5]. Hu X, Yu J, Qian C, Lu Y, Kahkoska AR, Xie Z, Jing X, Buse JB, Gu Z, H2O2 - Responsive Vesicles Integrated with Transcutaneous Patches for Glucose-Mediated Insulin Delivery, ACS Nano. 11 (2017) 613–620. 10.1021/acsnano.6b06892. [PubMed: 28051306]

[6]. Gupta R, Mohanty S, Controlled release of insulin from folic acid-insulin complex nanoparticles, Colloids Surfaces B Biointerfaces. 154 (2017) 48–54. 10.1016/j.colsurfb.2017.03.002. [PubMed: 28288342]

[7]. Choi S, Kim SW, Controlled release of insulin from injectable biodegradable triblock copolymer depot in ZDF rats., Pharm. Res 20 (2003) 2008–10. 10.1023/b:pham.0000008050.99985.5c. [PubMed: 14725367]

[8]. Polonsky WH, Henry RR, Poor medication adherence in type 2 diabetes: Recognizing the scope of the problem and its key contributors, Patient Prefer. Adherence 10 (2016) 1299–1306. 10.2147/PPA.S106821. [PubMed: 27524885]

[9]. Control Diabetes and Complications Trial Research, The Effect of Intensive Treatment of Diabetes on the Development and Progression of Long-Term Complications in Insulin-Dependent Diabetes Mellitus, N. Engl. J. Med 329 (1993) 977–986. [PubMed: 8366922]

[10]. Yang W, Dall TM, Beronjia K, Lin J, Semilla AP, Chakrabarti R, Hogan PF, Petersen MP, Economic costs of diabetes in the U.S., Diabetes Care. 41 (2017) 917–928. 10.2337/dci18-0007.

[11]. Zhang P, Gregg E, Global economic burden of diabetes and its implications., Lancet. Diabetes Endocrinol 5 (2017) 404–405. 10.1016/S2213-8587(17)30100-6. [PubMed: 28456417]

[12]. Standl E, New Long-Acting Basal Insulins: Does Benefit Outweigh Cost?, Diabetes Care. 39 (2016) S172–S179. https://care.diabetesjournals.org/content/diacare/39/Supplement_2/S172.full.pdf (accessed September 17, 2019). [PubMed: 27440830]

[13]. Al- Tahami K, Oak M, Mandke R, Singh J, Basal level insulin delivery: In vitro release, stability, biocompatibility, and in vivo absorption from thermosensitive triblock copolymers, J. Pharm. Sci 100 (2011) 4790–4803. 10.1002/jps.22685. [PubMed: 21713772]

[14]. Oak M, Singh J, Chitosan-zinc-insulin complex incorporated thermosensitive polymer for controlled delivery of basal insulin in vivo, J. Control. Release 163 (2012) 145–153. 10.1016/j.jconrel.2012.07.035. [PubMed: 22902516]

[15]. Chen S, Pederson D, Oak M, Singh J, In Vivo Absorption of Steroidal Hormones from Smart Polymer Based Delivery Systems, J. Pharm. Sci 99 (2010) 3381–3388. 10.1002/jps.22098. [PubMed: 20213838]

[16]. Liu J, Zhang SM, Chen PP, Cheng L, Zhou W, Tang WX, Chen ZW, Ke CM, Controlled release of insulin from PLGA nanoparticles embedded within PVA hydrogels, J. Mater. Sci. Mater. Med 18 (2007) 2205–2210. 10.1007/s10856-007-3010-0. [PubMed: 17668296]

[17]. Lipp L, Sharma D, Banerjee A, Singh J, Controlled Delivery of Salmon Calcitonin Using Thermosensitive Triblock Copolymer Depot for Treatment of Osteoporosis., ACS Omega. 4 (2019) 1157–1166. 10.1021/acsomega.8b02781. [PubMed: 30729223]

[18]. Bigrigg A, Evans M, Gbolade B, Newton J, Pollard L, Szarewski A, Thomas C, Walling M, Depo Provera. Position paper on clinical use, effectiveness and side effects., Br. J. Fam. Plann 25 (1999) 69–76. http://europepmc.org/abstract/med/10454658 (accessed September 20, 2019). [PubMed: 10454658]

[19]. Halpern V, Stalter RM, Owen DH, Dorflinger LJ, Lendvay A, Rademacher KH, Towards the development of a longer-acting injectable contraceptive: past research and current trends, Contraception. 92 (2015) 3–9. 10.1016/J.CONTRACEPTION.2015.02.014. [PubMed: 25746058]

[20]. Sharma D, Lipp L, Arora S, Singh J, Diblock and triblock copolymers of polylactide and polyglycolide, in: Mater Biomed. Eng, Elsevier, 2019: pp. 449–477. 10.1016/b978-0-12-816874-5.00013-x.

[21]. Kamaly N, Yameen B, Wu J, Farokhzad OC, Degradable Controlled-Release Polymers and Polymeric Nanoparticles: Mechanisms of Controlling Drug Release., Chem. Rev 116 (2016) 2602–63. 10.1021/acs.chemrev.5b00346. [PubMed: 26854975]

[22]. Luippold G, Bedenik J, Voigt A, Grempler R, Short- and Longterm Glycemic Control of Streptozotocin-Induced Diabetic Rats Using Different Insulin Preparations, PLoS One. 11 (2016) 1–12. 10.1371/journal.pone.0156346.

[23]. Sharma D, Singh J, Synthesis and Characterization of Fatty Acid Grafted Chitosan Polymer and Their Nanomicelles for Nonviral Gene Delivery Applications, Bioconjug. Chem 28 (2017) 2772–2783. 10.1021/acs.bioconjchem.7b00505. [PubMed: 29040803]

[24]. Sharma D, Arora S, Singh J, Smart thermosensitive copolymer incorporating chitosan-zinc-insulin electrostatic complexes for controlled delivery of insulin: effect of chitosan chain length, Int. J. Polym. Mater. Polym. Biomater (2019) 1–15. 10.1080/00914037.2019.1655750.

[25]. Hayton WL, Chen T, Correction of Perfusate Concentration for Sample Removal, J. Pharm. Sci 71 (1982) 820–821. 10.1002/jps.2600710726. [PubMed: 7120072]

[26]. Lin Y-C, Boone M, Meuris L, Lemmens I, Van Roy N, Soete A, Reumers J, Moisse M, Plaisance S, Drmanac R, Chen J, Speleman F, Lambrechts D, Van de Peer Y, Tavernier J, Callewaert N, Genome dynamics of the human embryonic kidney 293 lineage in response to cell biology manipulations, Nat. Commun 5 (2014) 4767 10.1038/ncomms5767. [PubMed: 25182477]

[27]. Aung MH, Kim MK, Olson DE, Thule PM, Pardue MT, Early visual deficits in streptozotocin-induced diabetic long evans rats, Investig. Ophthalmol. Vis. Sci 54 (2013) 1370–1377. 10.1167/iovs.12-10927. [PubMed: 23372054]

[28]. Muranov K, Poliansky N, Winkler R, Rieger G, Schmut O, Horwath-Winter J, Protection by iodide of lens from selenite-induced cataract, Graefe's Arch. Clin. Exp. Ophthalmol 242 (2004) 146–151. 10.1007/s00417-003-0790-x. [PubMed: 14658071]

[29]. Gyarmati B, Hegyesi N, Pukánszky B, Szilágyi A, A colourimetric method for the determination of the degree of chemical cross-linking in aspartic acid-based polymer gels, Express Polym. Lett 9 (2015) 154–164. 10.3144/expresspolymlett.2015.16.

[30]. Cayot P, Tainturier G, The quantification of protein amino groups by the trinitrobenzenesulfonic acid method: A reexamination, Anal. Biochem 249 (1997) 184–200. 10.1006/abio.1997.2161. [PubMed: 9212870]

[31]. Vinther TN, Norrman M, Strauss HM, Huus K, Schlein M, Pedersen TA, Kjeldsen T, Jensen KJ, Hubálek F, Novel covalently linked insulin dimer engineered to investigate the function of insulin dimerization, PLoS One. 7 (2012) 1–9. 10.1371/journal.pone.0030882.

[32]. Huus K, Havelund S, Olsen HB, Van De Weert M, Frokjaer S, Thermal dissociation and unfolding of insulin, Biochemistry. 44 (2005) 11171–11177. 10.1021/bi0507940. [PubMed: 16101301]

[33]. Iwai W, Yamada T, Kurihara K, Ohnishi Y, Kobayashi Y, Tanaka I, Takahashi H, Kuroki R, Tamada T, Niimura N, A neutron crystallographic analysis of T6 porcine insulin at 2.1 A resolution., Acta Crystallogr. D. Biol. Crystallogr 65 (2009) 1042–50. 10.1107/S090744490902770X. [PubMed: 19770501]

[34]. Jeong B, Bae YH, Kim SW, Drug release from biodegradable injectable thermosensitive hydrogel of PEG–PLGA–PEG triblock copolymers, J. Control. Release 63 (2000) 155–163. 10.1016/S0168-3659(99)00194-7. [PubMed: 10640589]

[35]. Brange J, Andersen L, Laursen ED, Meyn G, Rasmussen E, Toward Understanding Insulin Fibrillation, J. Pharm. Sci 86 (1997) 517–525. 10.1021/JS960297S. [PubMed: 9145374]

[36]. Hua QX, Jia W, Weiss MA, Conformational dynamics of insulin, Front. Endocrinol. (Lausanne) 2 (2011) 1–11. 10.3389/fendo.2011.00048. [PubMed: 22649356]

[37]. Brange J, Langkjoer L, Insulin structure and stability., Pharm. Biotechnol 5 (1993) 315–50. http://www.ncbi.nlm.nih.gov/pubmed/8019699 (accessed November 29, 2018). [PubMed: 8019699]

[38]. Xu Y, Yan Y, Seeman D, Sun L, Dubin PL, Multimerization and aggregation of native-state insulin: Effect of zinc, Langmuir. 28 (2012) 579–586. 10.1021/la202902a. [PubMed: 22059434]

[39]. Kelly SM, Price NC, The Use of Circular Dichroism in the Investigation of Protein Structure and Function, Curr. Protein Pept. Sci 1 (2000) 349–384. https://ctrstbio.org.uic.edu/manuals/kelly.pdf (accessed July 6, 2018). [PubMed: 12369905]

[40]. Tang Y, Singh J, Thermosensitive drug delivery system of salmon calcitonin: In vitro release, in vivo absorption, bioactivity and therapeutic efficacies, Pharm. Res 27 (2010) 272–284. 10.1007/s11095-009-0015-z. [PubMed: 19998055]

[41]. Tang Y, Singh J, Biodegradable and biocompatible thermosensitive polymer based injectable implant for controlled release of protein, Int. J. Pharm 365 (2009) 34–43. 10.1016/j.ijpharm.2008.08.018. [PubMed: 18786623]

[42]. Manoharan C, Singh J, Evaluation of polyanhydride microspheres for basal insulin delivery: Effect of copolymer composition and zinc salt on encapsulation, in vitro release, stability, in vivo absorption and bioactivity in diabetic rats, J. Pharm. Sci 98 (2009) 4237–4250. 10.1002/jps.21741. [PubMed: 19472196]

[43]. Oak M, Singh J, Controlled delivery of basal level of insulin from chitosan-zinc-insulin-complex-loaded thermosensitive copolymer., J. Pharm. Sci 101 (2012) 1079–96. 10.1002/jps.22823. [PubMed: 22095295]

[44]. Ellis MJ, Darby SC, Jones RH, Sonksen PH, In Vitro Bioactivity of Insulin Analogues: Lipogenic and Anti-Lipolytic Potency and Their Interaction with the Effect of Native Insulin, Diabetologia. 15 (1978) 403–410. [PubMed: 738550]

[45]. Makadia HK, Siegel SJ, Poly Lactic-co-Glycolic Acid (PLGA) as biodegradable controlled drug delivery carrier, Polymers (Basel). 3 (2011) 1377–1397. 10.3390/polym3031377. [PubMed: 22577513]

[46]. Ulery BD, Nair LS, Laurencin CT, Biomedical applications of biodegradable polymers, J. Polym. Sci. Part B Polym. Phys 49 (2011) 832–864. 10.1002/polb.22259.

[47]. Kucharczyk P, Pavelková A, Stloukal P, Sedlarík V, Degradation behaviour of PLA-based polyesterurethanes under abiotic and biotic environments, Polym. Degrad. Stab 129 (2016) 222–230. 10.1016/j.polymdegradstab.2016.04.019.

[48]. Mei T, Zhu Y, Ma T, He T, Li L, Wei C, Xu K, Synthesis, characterization, and biocompatibility of alternating block polyurethanes based on PLA and PEG, J. Biomed. Mater. Res. - Part A 102 (2014) 3243–3254. 10.1002/jbm.a.35004.

[49]. Elsawy MA, Kim KH, Park JW, Deep A, Hydrolytic degradation of polylactic acid (PLA) and its composites, Renew. Sustain. Energy Rev 79 (2017) 1346–1352. 10.1016/j.rser.2017.05.143.

[50]. Straus DS, Effects of insulin on cellular growth and proliferation, Life Sci. 29 (1981) 2131–2139. 10.1016/0024-3205(81)90482-3. [PubMed: 7033701]

[51]. Li YV, Zinc and insulin in pancreatic beta-cells, Endocrine. 45 (2014) 178–189. 10.1007/s12020-013-0032-x. [PubMed: 23979673]

[52]. Teng D, From Chitin to Chitosan, in: Yao K, Li J, Yao F, Yin Y (Eds.), Chitosan-Based Hydrogels Funct. Appl, CRC Press, 2017: p. 521 https://books.google.com/books?id=OlPRBQAAQBAJ&pg=PA415&lpg=PA415&dq=chitosan+helps+in+cell+proliferation+and+attachment&source=bl&ots=E9czI1NM4d&sig=_xYcNK9MzBKd1max-6h0lqFDlDk&hl=en&sa=X&ved=0ahUKEwjEtHc_YrcAhVE0oMKHR0mAUMQ6AEIUzAG#v=onepage&q=chitosan.

[53]. Ignatius AAA, Claes LEE, In vitro biocompatibility of bioresorbable polymers: poly(L, DL-lactide) and poly(L-lactide-co-glycolide), Biomaterials. 17 (1996) 831–839. 10.1016/0142-9612(96)81421-9. [PubMed: 8730968]

[54]. Onuki Y, Bhardwaj U, Papadimitrakopoulos F, Burgess DJ, A review of the biocompatibility of implantable devices: current challenges to overcome foreign body response., J. Diabetes Sci. Technol 2 (2008) 1003–15. 10.1177/193229680800200610. [PubMed: 19885290]

[55]. Veronese FM, Pasut G, PEGylation, successful approach, 10 (2005) 1451–1458. 10.1016/S1359-6446(05)03575-0.

[56]. Wake MC, Gupta PK, Mikos AG, Fabrication of pliable biodegradable polymer foams to engineer soft tissues., Cell Transplant. 5 (1996) 465–73. http://www.ncbi.nlm.nih.gov/pubmed/8800514 (accessed November 29, 2018). [PubMed: 8800514]

[57]. Bonacucina G, Cespi M, Mencarelli G, Giorgioni G, Palmieri GF, Thermosensitive self-assembling block copolymers as drug delivery systems, Polymers (Basel). 3 (2011) 779–811. 10.3390/polym3020779.

[58]. Chamberlain JJ, Kalyani RR, Leal S, Rhinehart AS, Shubrook JH, Skolnik N, Herman WH, Treatment of Type 1 Diabetes: Synopsis of the 2017 American Diabetes Association Standards of Medical Care in Diabetes, Ann. Intern. Med 167 (2017) 493 10.7326/M17-1259. [PubMed: 28892816]

[59]. Matejko B, Kukułka A, Kieć-Wilk B, Stąpór A, Klupa T, Malecki MT, Basal Insulin Dose in Adults with Type 1 Diabetes Mellitus on Insulin Pumps in Real-Life Clinical Practice: A Single-Center Experience., Adv. Med 2018 (2018) 1473160 10.1155/2018/1473160. [PubMed: 29974056]

[60]. N.C.G.C. (UK), Type 1 Diabetes in Adults: Diagnosis and Management, National Institute for Health and Care Excellence (UK), 2015 http://www.ncbi.nlm.nih.gov/pubmed/26334079 (accessed September 18, 2019).

[61]. Xun P, Liu K, Cao W, Sidney S, Williams OD, He K, Fasting Insulin Level Is Positively Associated With Incidence of Hypertension Among American Young Adults: A 20-year follow-up study, Diabetes Care. 35 (2012) 1532–1537. 10.2337/dc11-2443. [PubMed: 22511258]

[62]. Heise T, Pieber TR, Towards peakless, reproducible and long-acting insulins. An assessment of the basal analogues based on isoglycaemic clamp studies, Diabetes, Obes. Metab 9 (2007) 648–659. 10.1111/j.1463-1326.2007.00756.x.

[63]. Eliaschewitz FG, Barreto T, Concepts and clinical use of ultra-long basal insulin., Diabetol. Metab. Syndr 8 (2016) 1–8. 10.1186/s13098-015-0117-1. [PubMed: 26734075]

[64]. Jeong B, Bae YH, Kim SW, Drug release from biodegradable injectable thermosensitive hydrogel of PEG-PLGA-PEG triblock copolymers., J. Control. Release 63 (2000) 155–63. 10.1016/s0168-3659(99)00194-7. [PubMed: 10640589]

[65]. Hildebrandt P, Subcutaneous absorption of insulin in insulin-dependent diabetic patients. Influence of species, physico-chemical properties of insulin and physiological factors., Dan. Med. Bull 38 (1991) 337–46. http://www.ncbi.nlm.nih.gov/pubmed/1914533 (accessed September 18, 2019). [PubMed: 1914533]

[66]. Kang S, Brange J, Burch A, Volund A, Owens DR, Subcutaneous Insulin Absorption Explained by Insulin's Physicochemical Properties: Evidence From Absorption Studies of Soluble Human Insulin and Insulin Analogues in Humans, Diabetes Care. 14 (1991) 942–948. 10.2337/diacare.14.11.942. [PubMed: 1797506]

[67]. Jiráček J, Žáková L, Antolíková E, Watson CJ, Turkenburg JP, Dodson GG, Brzozowski AM, Implications for the active form of human insulin based on the structural convergence of highly active hormone analogues, Proc. Natl. Acad. Sci. U. S. A 107 (2010) 1966–1970. 10.1073/pnas.0911785107. [PubMed: 20133841]

[68]. Lodhi G, Kim Y-S, Hwang J-W, Kim S-K, Jeon Y-J, Je J-Y, Ahn C-B, Moon S-H, Jeon B-T, Park P-J, Chitooligosaccharide and its derivatives: preparation and biological applications., Biomed Res. Int 2014 (2014) 654913 10.1155/2014/654913. [PubMed: 24724091]

[69]. Mukherjee S, Mondal S, Deshmukh AA, Gopal B, Bagchi B, What Gives an Insulin Hexamer Its Unique Shape and Stability? Role of Ten Confined Water Molecules, J. Phys. Chem. B 122 (2018) 1631–1637. 10.1021/acs.jpcb.8b00453. [PubMed: 29341613]

[70]. Mitchell HH, The effect of the proportions of fat and carbohydrate in the diet upon the excretion of metabolic nitrogen in the feces, J. Biol. Chem (1934). http://www.jbc.org/ (accessed February 27, 2020).

[71]. Koch MA, Experimental Modeling and Research Methodology, in: Lab. Rat, Second, Academic Press, 2006: pp. 587–625. 10.1016/B978-012074903-4/50021-2.

[72]. Dhatariya K, Blood Ketones: Measurement, Interpretation, Limitations, and Utility in the Management of Diabetic Ketoacidosis., Rev. Diabet. Stud 13 (2016) 217–225. 10.1900/RDS.2016.13.217. [PubMed: 28278308]

[73]. Elsner M, Guldbakke B, Tiedge M, Munday R, Lenzen S, Relative importance of transport and alkylation for pancreatic beta-cell toxicity of streptozotocin, Diabetologia. 43 (2000) 1528–1533. 10.1007/s001250051564. [PubMed: 11151762]

[74]. Szkudelski T, The mechanism of alloxan and streptozotocin action in B cells of the rat pancreas., Physiol. Res 50 (2001) 537–46. http://www.ncbi.nlm.nih.gov/pubmed/11829314 (accessed September 21, 2019). [PubMed: 11829314]

[75]. Fineberg SE, Kawabata TT, Finco-Kent D, Fountaine RJ, Finch GL, Krasner AS, Immunological Responses to Exogenous Insulin, Endocr. Rev 28 (2007) 625–652. 10.1210/er.2007-0002. [PubMed: 17785428]

[76]. Baker M, Reynolds HM, Lumicisi B, Bryson CJ, Immunogenicity of protein therapeutics: The key causes, consequences and challenges, Self. Nonself 1 (2010) 314–322. 10.4161/self.1.4.13904. [PubMed: 21487506]

Highlights

- Chitosan stabilizes hexameric insulin structure by electrostatic complex formation
- Hydrophobic complexes show slow diffusion from thermogel copolymer matrix
- Thermogel copolymers form *in situ* gel depot upon subcutaneous injection
- Sustained insulin release from thermogel depot prevents diabetes complications

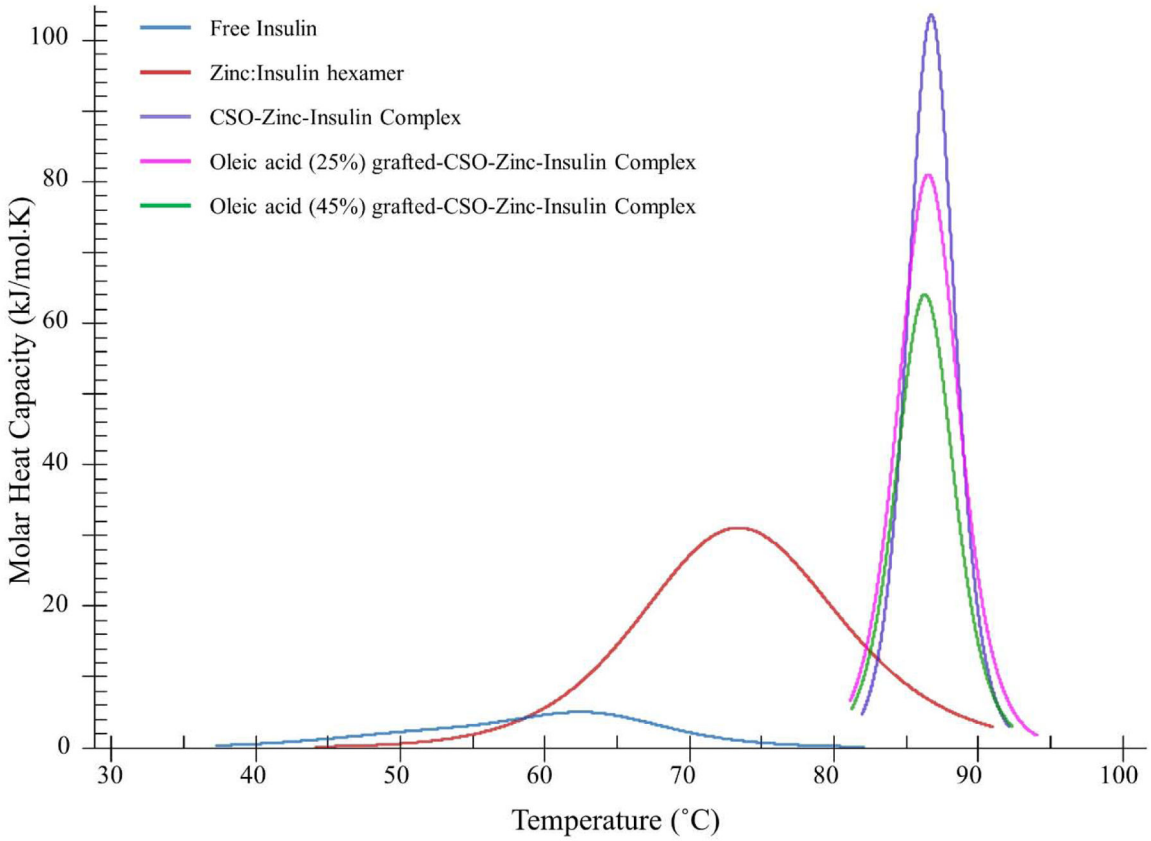

Figure 1.

Differential scanning calorimetry thermogram of insulin, zinc-insulin hexamers and chitosan-zinc-insulin complexes prepared using oleic acid-grafted chitosan polymers. [Insulin: 1 mg/mL; Zinc ions: insulin hexamer (1:5); CSO monomer unit: insulin monomer (5:1); in phosphate buffered saline (10 mM, pH 7.4)]

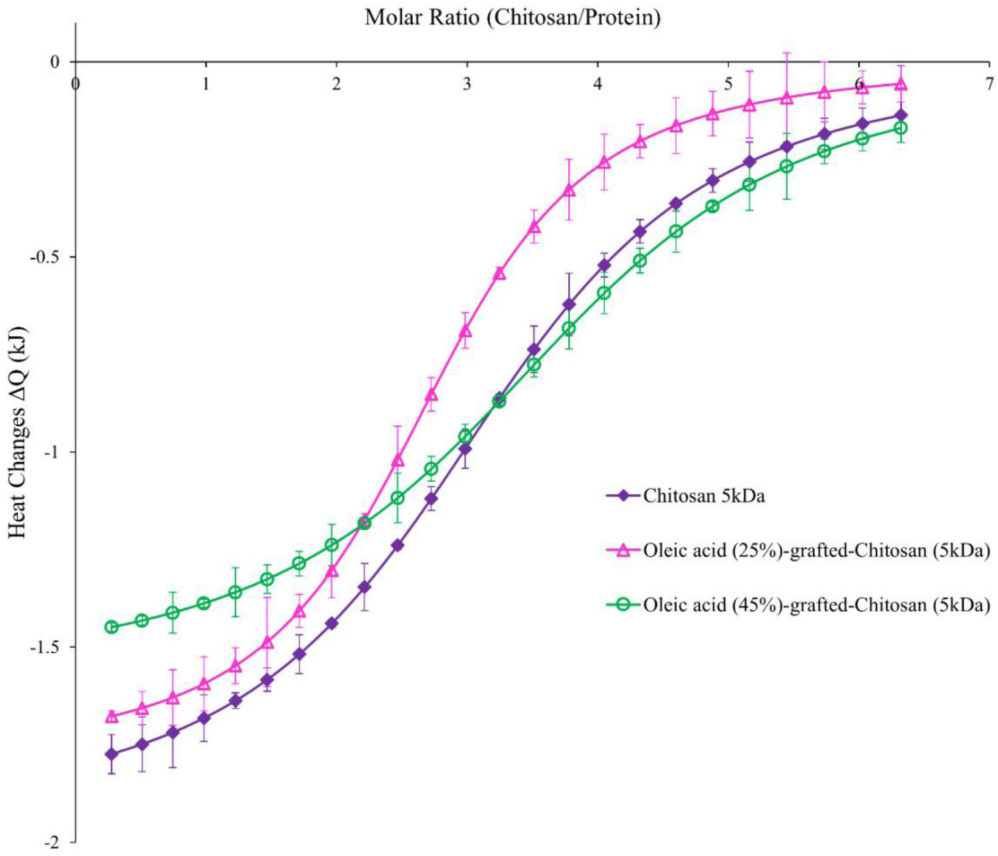

Figure 2.

Integrated heats of interaction from calorimetric titrations of oleic acid grafted chitosan polymer (titrant) into zinc-insulin hexamers (titrand). [2 mg/mL, ~0.057 mM zinc-insulin hexamers; 1.2 mg/mL, CSO polymer solution; in phosphate buffered saline (10 mM, pH 7.4)] Data are expressed as mean ± S.D, n=3.

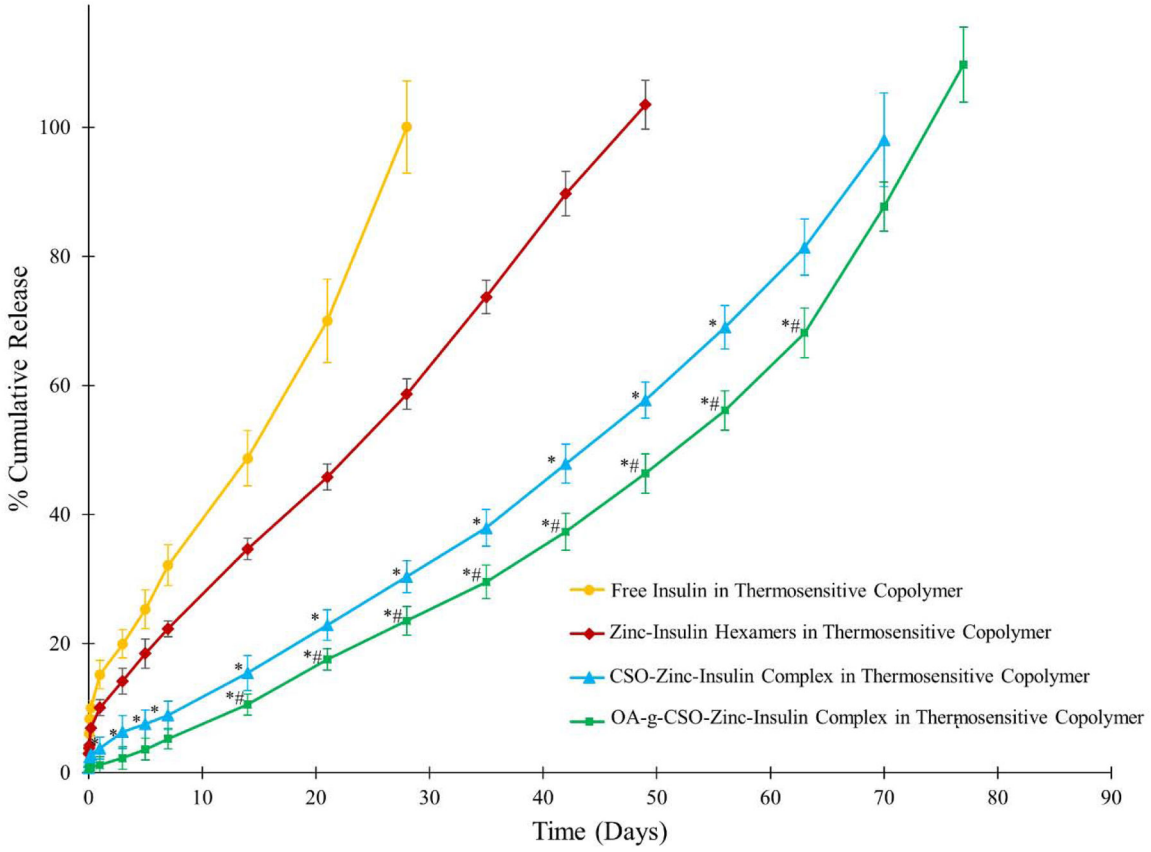

Figure 3.

Effect of hydrophobic modification on chitosan oligosaccharide (CSO, 5 kDa) on *in vitro* release of insulin from 35% (w/v) PLA_{1500}-PEG_{1500}-PLA_{1500} copolymer, drug loading: 0.15% (w/v). Data is expressed as mean ± SD, n=4. [Key: (●) free insulin, (◆) zinc-insulin hexamers, (▲) CSO-zinc-insulin complex, (■) oleic $acid_{(45\%)}$-grafted-CSO-zinc-insulin complex; *: significantly lower compared to zinc-insulin hexamers; #: significantly lower compared to CSO-zinc-insulin complex; at $p < 0.05$]

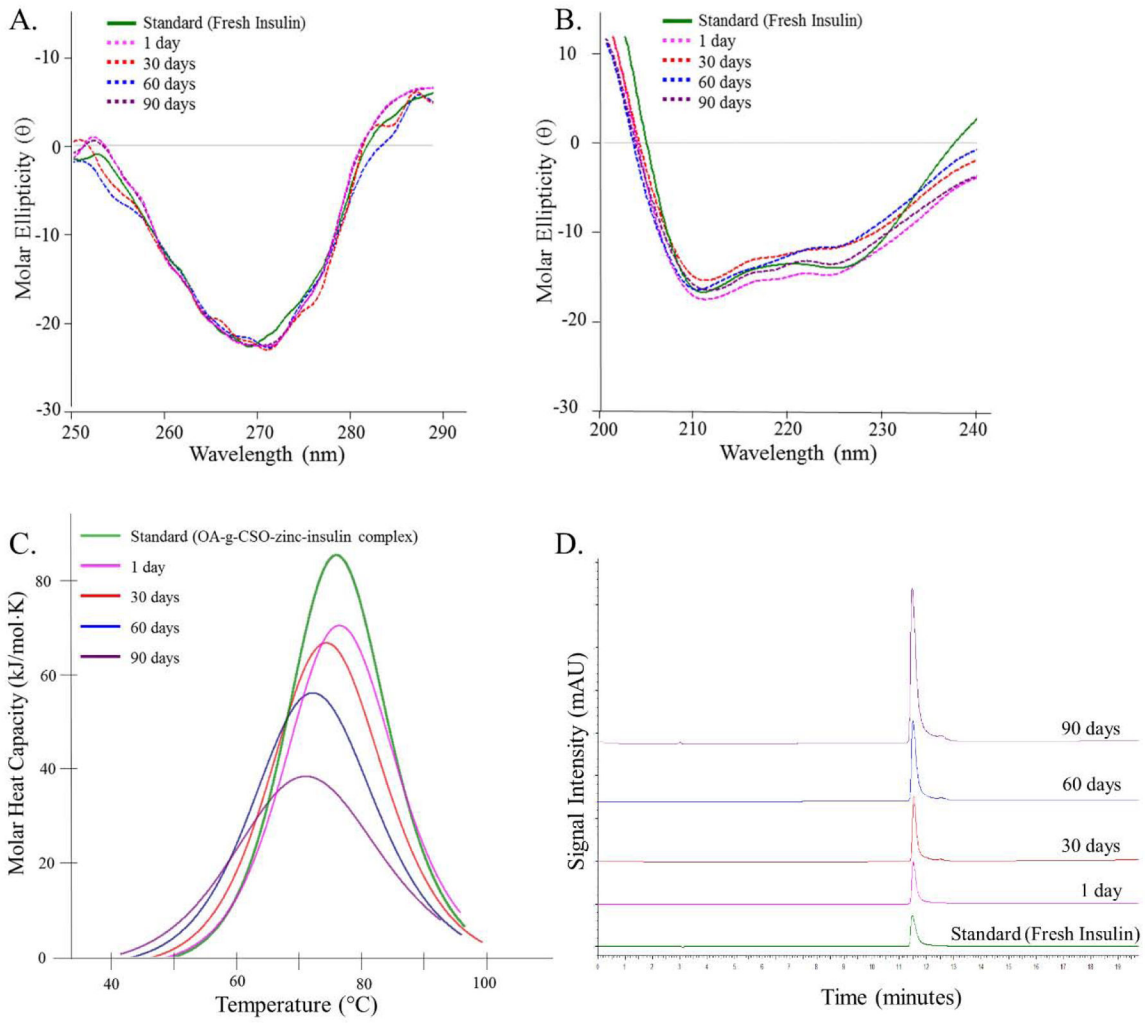

Figure 4.

(A) Near-UV circular dichroism spectrum, (B) Far-UV circular dichroism spectrum, (C) Nano-differential scanning calorimetry fitted thermogram, and (D) Reversed phase high performance liquid chromatography, of insulin released *in vitro* at 1, 30, 60 and 90 days from OA-g-CSO-zinc-insulin complexes incorporated in thermosensitive copolymer formulation at 37 °C. [Key: green - standard solution, pink - one day, red - 30 days, blue - 60 days, and purple - 90 days, on stability analysis at 37 °C.]

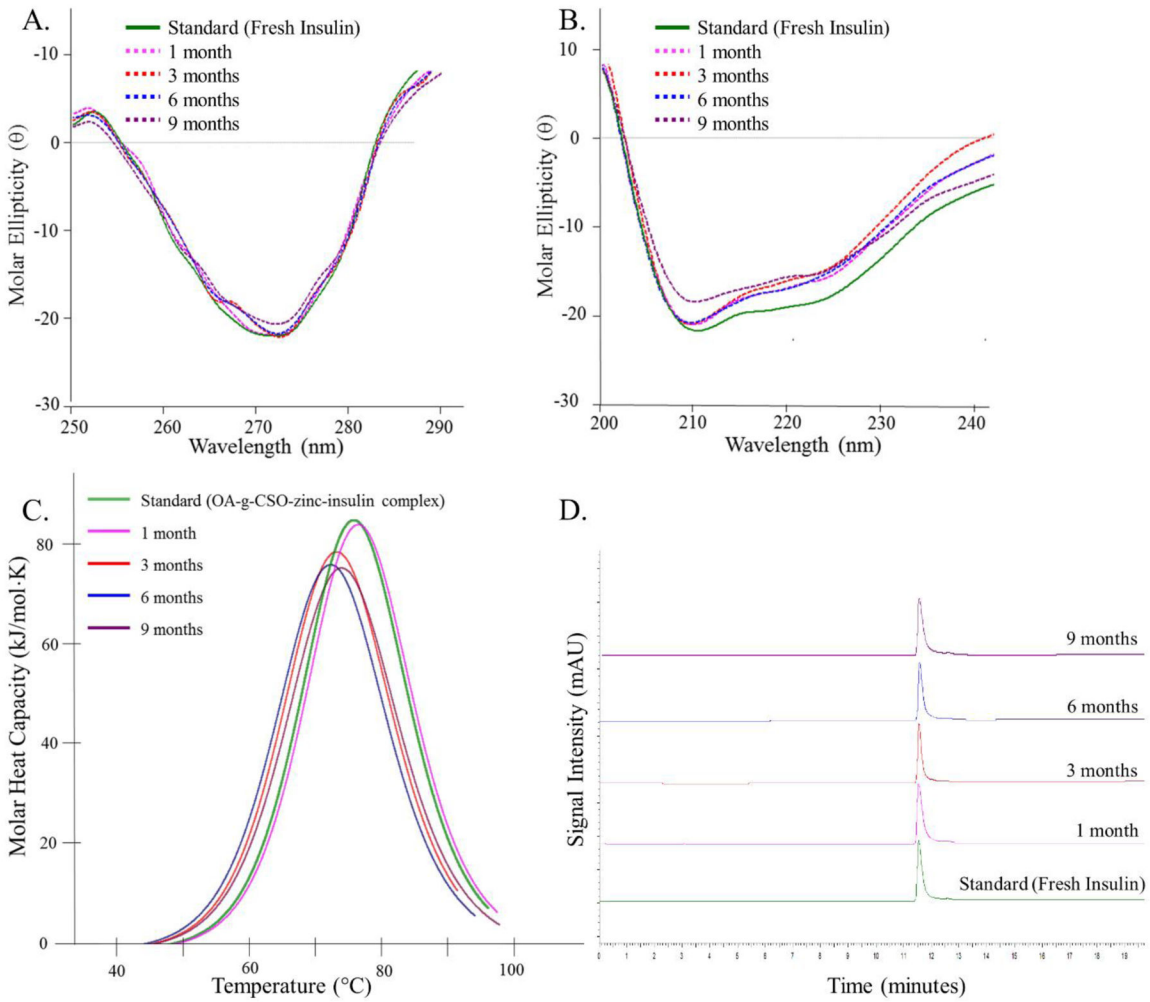

Figure 5.

(A) Near-UV circular dichroism spectrum, (B) Far-UV circular dichroism spectrum, (C) Nano-differential scanning calorimetry fitted thermogram, and (D) Reversed phase high performance liquid chromatography, of insulin extracted from OA-g-CSO-zinc-insulin complexes incorporated in thermosensitive copolymer formulation after 1, 3, 6 and 9 months of storage at 4 °C. [Key: green - standard solution, pink - one month, red - 3 months, blue - 6 months, and purple - 9 months, on stability analysis at 4 °C.]

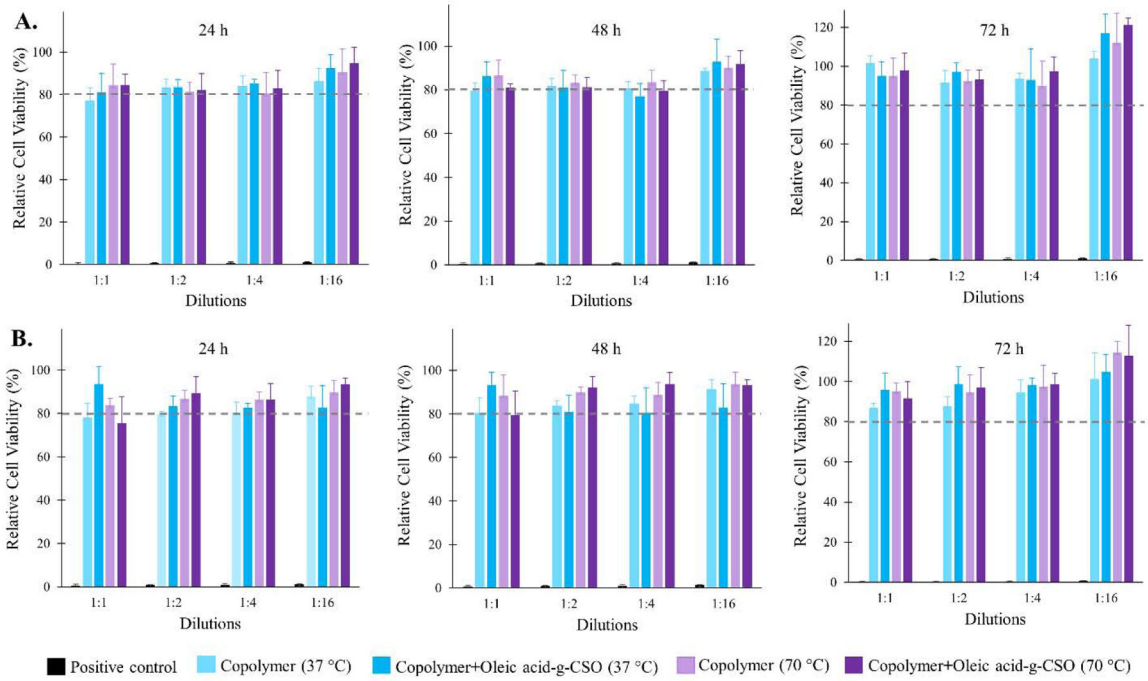

Figure 6.

Graphical representation of percent relative cell viability after 24, 48 and 72 h at different dilutions of copolymer degradation products incubated with (A) 3T3–L1 fibroblast cell line (B) HEK 293 cell line. Thermosensitive copolymer PLA-PEG-PLA incorporating oleic acid-g-CSO polymer was incubated with PBS for 10 days at 37 °C to extract the copolymer, CSO polymer and their degradation products. Biocompatibility was evaluated using MTT assay. Positive control (formalin) showed ≤ 1.0 ± 0.2 % relative cell viability at the highest dilution (1:16) in cell culture medium, and negligible cell survival at lowest dilution (1:1) in cell culture medium for both 3T3–L1 and HEK 293 cell lines. Data expressed as mean ± SD, n = 4.

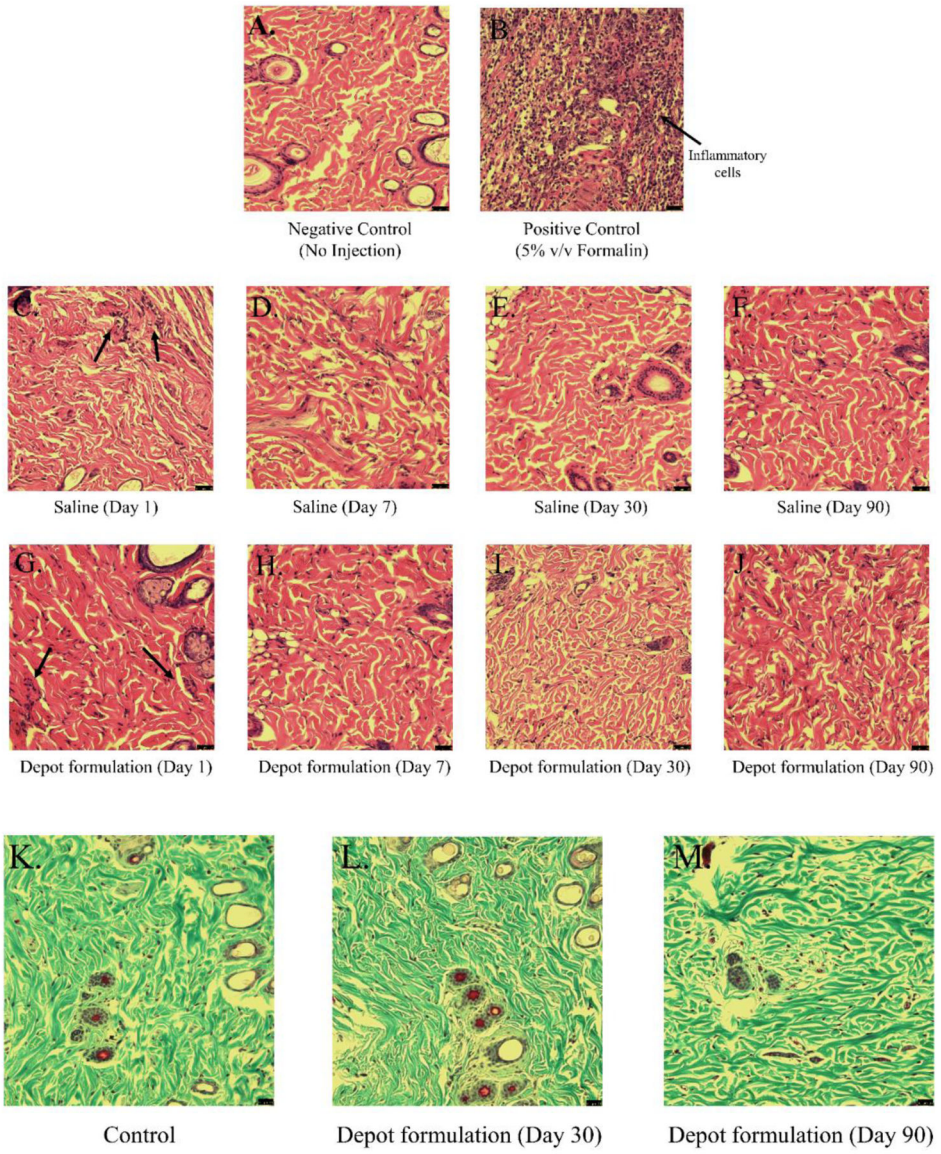

Figure 7.

Bright field micrographs of H & E stained rat injection site skin tissue after (A) no injection (negative control), (B) 5% (v/v) Formalin (positive control), (C – F) 1, 7, 30 and 90 days' post administration of Saline, (G – J) 1, 7, 30 and 90 days' post administration of OA-g-CSO incorporated in thermosensitive copolymer formulation. Bright field micrographs of Gomori's trichome stained rat injection site skin tissue after (K) no injection, and (L) 30 days, (M) 90 days, post administration of OA-g-CSO incorporated in thermosensitive copolymer formulation.

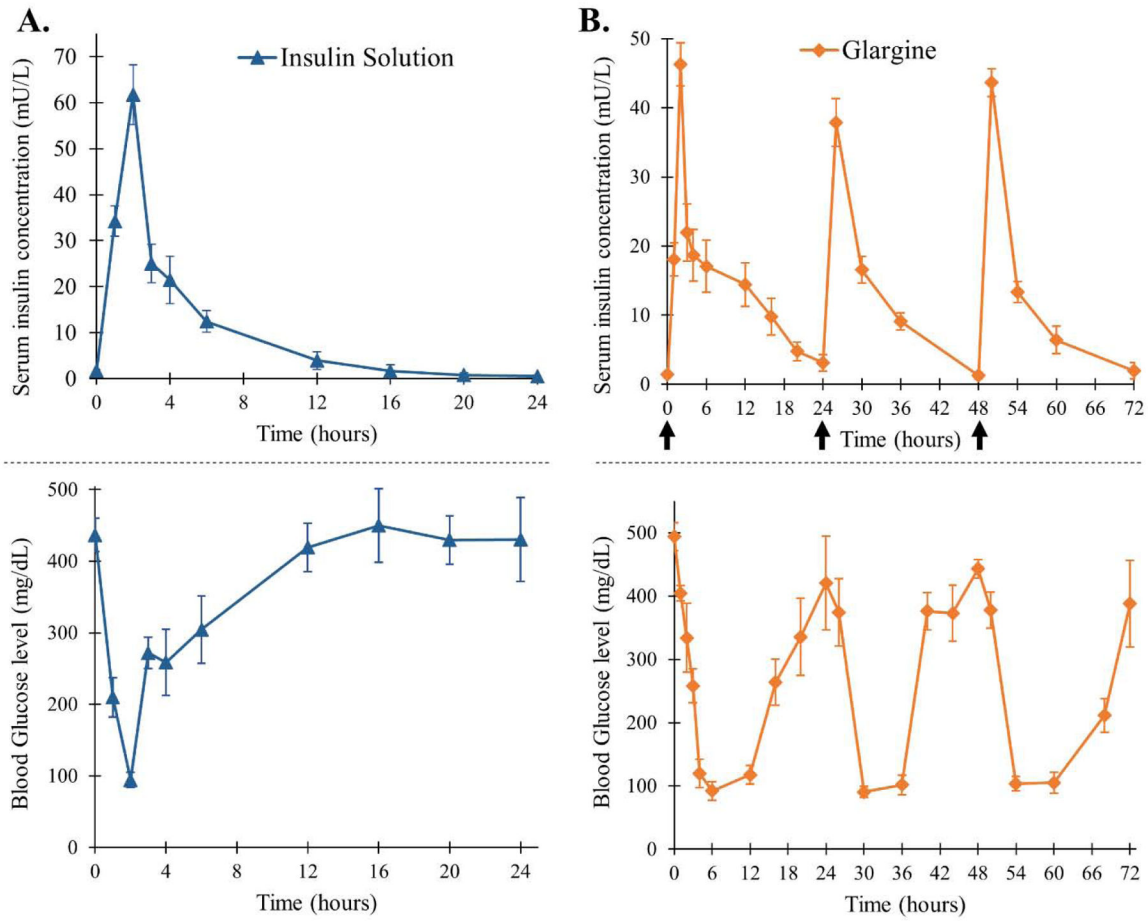

Figure 8.

Serum insulin concentration and blood glucose level of STZ-induced diabetic rats upon treatment with (A) single administration of recombinant human insulin and (B) daily administration of insulin glargine (Lantus® U-100). [Data are expressed as mean ± S.D, n=6; arrows mark administration of glargine; insulin dose: 0.5 IU/kg/day]

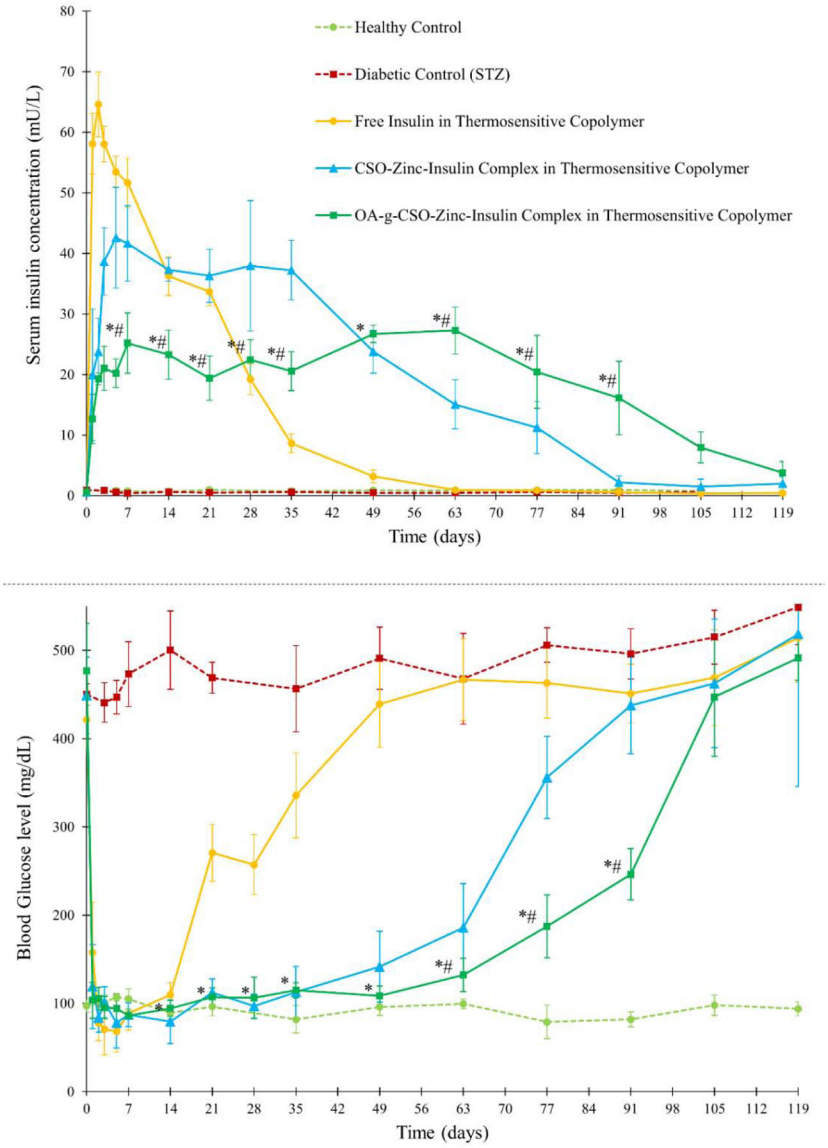

Figure 9.

Serum insulin concentration and blood glucose level of STZ-induced diabetic rats upon insulin treatment. Key: Treatment with single administration of: (●) free insulin in thermosensitive copolymer, dose 45 IU/kg; (▲) CSO-zinc-insulin complex in thermosensitive copolymer, dose 45 IU/kg; or (■) oleic acid$_{(45\%)}$-grafted-CSO-zinc-insulin complex in thermosensitive copolymer, dose 45 IU/kg; (■) untreated STZ-induced diabetic control; (●) healthy non-diabetic control. [Data are expressed as mean ± S.D, n=6; *: significantly different compared to glargine treated control; #: significantly different compared to CSO-zinc-insulin complex; at $p < 0.05$]

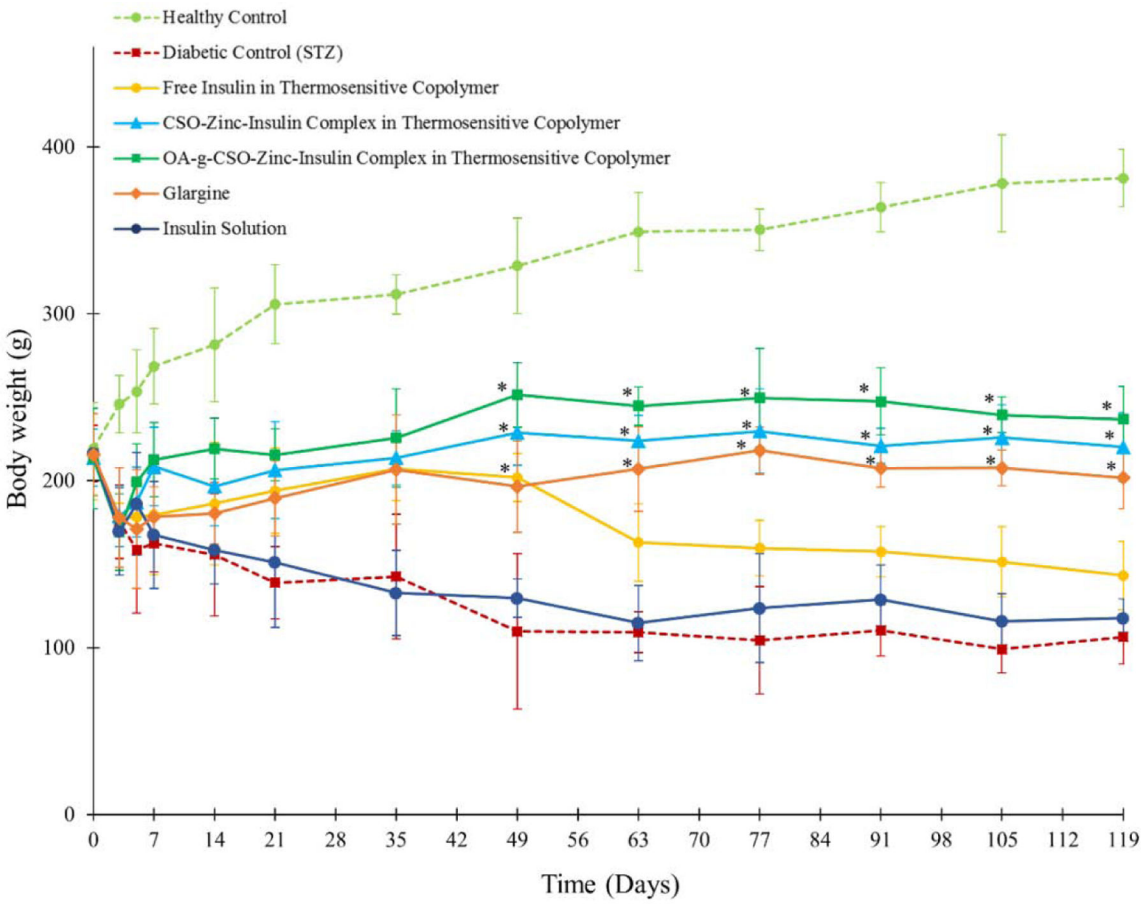

Figure 10.

Body weight of rats following STZ and insulin treatment. Key: (●) healthy non-diabetic control; (■) untreated STZ-induced diabetic control; STZ-induced diabetic rats upon treatment with single administration of: (●) insulin solution, dose 0.5 IU/kg; (●) free insulin in thermosensitive copolymer, dose 45 IU/kg; (▲) CSO-zinc-insulin complex in thermosensitive copolymer, dose 45 IU/kg; and (■) oleic acid$_{(45\%)}$-grafted-CSO-zinc-insulin complex in thermosensitive copolymer, dose 45 IU/kg; or (◆) daily administration of glargine (Lantus® U-100), dose 0.5 IU/kg/day. [Data are expressed as mean ± S.D, n=6; *: significantly higher compared to untreated STZ-induced diabetic control; at $p < 0.01$]

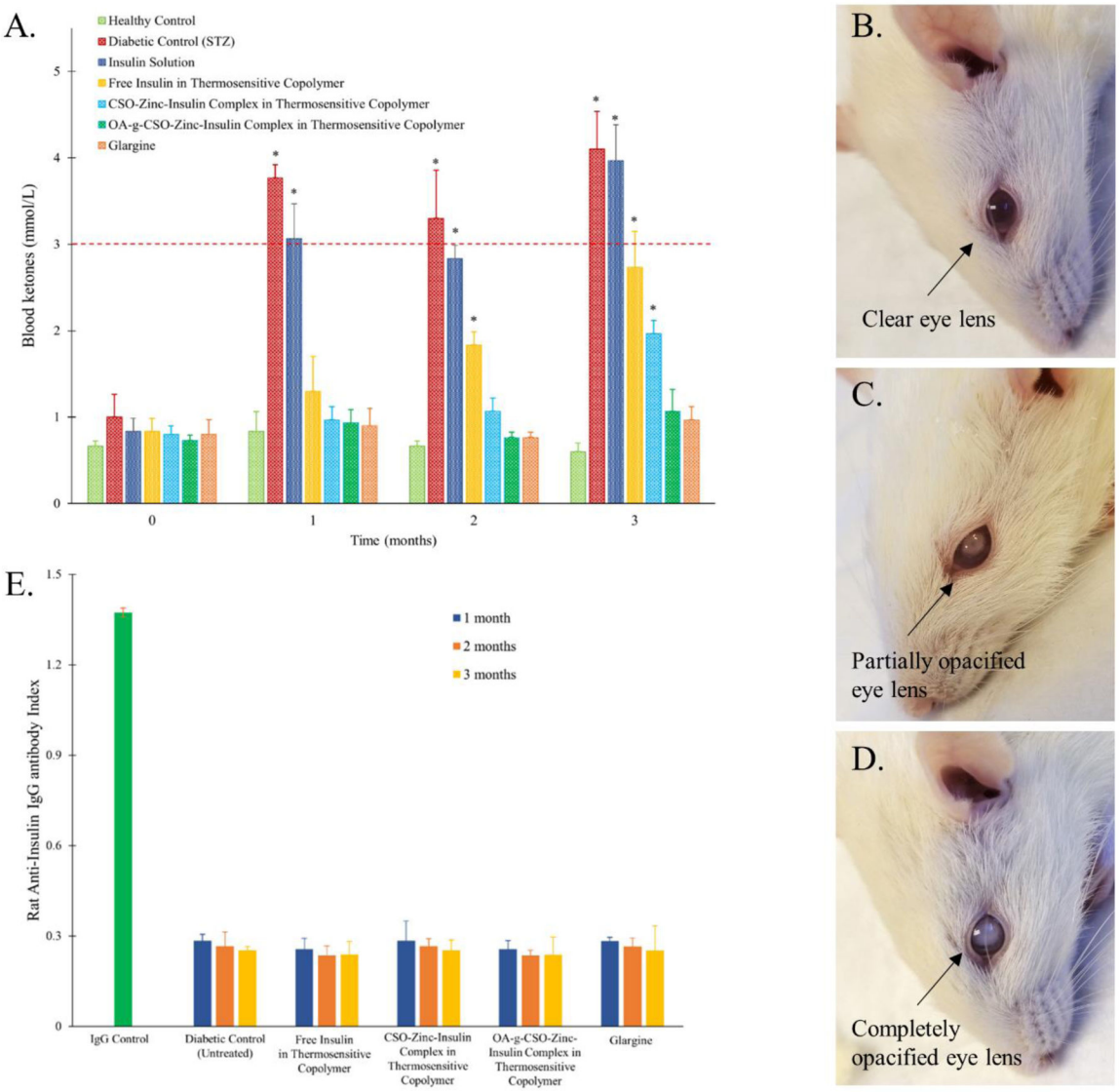

Figure 11.

(A) Blood ketone level in rats following STZ and insulin treatment; (B) Clear eye lens following treatment with oleic acid$_{(45\%)}$-grafted-CSO-zinc-insulin complex in thermosensitive copolymer; (C) Partial, or (D) total, cataract formation in untreated STZ-induced diabetic control; (E) Detection of anti-insulin antibodies following insulin treatment. Key: (●) healthy non-diabetic control; (■) untreated STZ-induced diabetic control; STZ-induced diabetic rats upon treatment with single administration of: (●) insulin solution, dose 0.5 IU/kg; (●) free insulin in thermosensitive copolymer, dose 45 IU/kg; (■) CSO-zinc-insulin complex in thermosensitive copolymer, dose 45 IU/kg; and (▲) oleic acid$_{(45\%)}$-grafted-CSO-zinc-insulin complex in thermosensitive copolymer, dose 45 IU/kg; or (◆) daily administration of glargine (Lantus® U-100), dose 0.5 IU/kg/day. [Data are expressed as mean ± S.D, n=6; *: significantly higher compared to healthy non-diabetic control; at $p < 0.05$]

Table 1.

Thermosensitive copolymeric formulations for studying *in vitro* release profile of insulin.

S. no.	Formulation	Insulin (mg/ mL of thermosensitive copolymer solution (35 % w/v))
1	Free insulin	0.63
2	Zinc-insulin hexamers	0.63
3	CSO (5 kDa)-zinc-insulin complexes	0.63
4	Oleic acid-g-CSO (5 kDa)-zinc-insulin complexes	0.63

Table 2.

Chromatographic conditions for studying chemical stability of insulin using RP-HPLC.

Column	Thermo Scientific™ Hypersil GOLD™ C18 column (250 × 4.6 mm, 5 μm)
Mobile phase A	0.1% v/v TFA in deionized water
Mobile phase B	0.1% v/v TFA in acetonitrile
Elution	Gradient
Mobile phase composition	75:25 (A:B) to 50:50 (A:B)
Flow rate	0.8 ml/min
Injection volume	25 μl
Run time	25 min
Detector, Detection wavelength	UV, 280 nm

Table 3.

Treatment groups for studying *in vivo* release profile of insulin.

Group number	Treatment	Insulin dose (IU/kg)	Frequency of administration
I	Healthy control	-	-
II	Diabetic control	-	-
III	Free insulin solution	0.5 IU/kg	Single
IV	Glargine	0.5 IU/kg/day	Repeated every 24 h
V	Free insulin in thermosensitive copolymer solution	45 IU/kg	Single
VI	CSO-Zinc insulin complexes in thermosensitive copolymer solution	45 IU/kg	Single
VII	Oleic acid-g-CSO zinc insulin complexes in thermosensitive copolymer solution	45 IU/kg	Single

Table 4.

Midpoint transition temperature (Tm) and transition enthalpy (ΔH) of insulin, zinc-insulin hexamers and chitosan-zinc-insulin complexes prepared using oleic acid-grafted chitosan polymers, in phosphate buffered saline at pH 7.4. Data are expressed as mean ± S.D, n=3.

Sample	Tm_1 (°C)	Tm_2 (°C)	AH (kJ/mol)
Insulin	51.87 ± 0.23	62.81 ± 0.29	97.27 ± 0.44
Zinc-Insulin hexamers	72.57 ± 0.19	-	344.15 ± 0.62
CSO (5 kDa) –Zinc-Insulin complex	86.73 ± 0.07	-	572.88 ± 4.33
Oleic acid (25%)-g-CSO-Zinc-Insulin complexes	86.53± 0.17	-	459.53 ± 5.29
Oleic acid (45%)-g-CSO-Zinc-Insulin complexes	86.30 ± 0.10	-	449.51 ± 3.21

Table 5.

Thermodynamic parameters of the binding interaction between oleic acid-grafted-chitosan polymers and zinc-insulin hexamers in phosphate buffered saline (10 mM, pH 7.4). Data are expressed as mean ± S.D, n=3.

Polymer	$k \times 10^7$ (M^{-1})	n (mol)	ΔH (kJ mol^{-1})
Chitosan 5 kDa (CSO)	11.17 ± 0.09	3.04 ± 0.09	−25.75 ± 0.87
CSO-g-Oleic acid (25%)	10.72 ± 0.27	3.26 ± 0.02	−23.96 ± 0.39
CSO-g-Oleic acid (45%)	9.99 ± 0.18	3.76 ± 0.01	−21.13 ± 0.12

Table 6.

Summary of total cataract formation following STZ and insulin treatment in Sprague Dawley rats.

	CATARACT FORMATION			
	60 days		90 days	
Group	**one eye**	**both eyes**	**one eye**	**both eyes**
Healthy control	0	0	0	0
Diabetic control (STZ) (untreated)	1	4	-	**6**
Insulin solution	3	2	1	**5**
Free Insulin in copolymeric depot	4	1	2	4
CSO-Zinc-Insulin complex in copolymeric depot	1	0	2	0
Oleic acid-g-CSO-Zinc-Insulin complex in copolymeric depot	0	0	0	0
Glargine	0	0	1	0